



Mears, E. M., Rossi, V., MacDonald, E., Coleman, G., Davies, T. G., Arias-Riesgo, C., Hildebrandt, C., Thiel, H., Duffin, C. J., Whiteside, D. I., & Benton, M. J. (2016). The Rhaetian (Late Triassic) vertebrates of Hampstead Farm Quarry, Gloucestershire, UK. *Proceedings of the Geologists' Association*, 127(4), 478-505.
<https://doi.org/10.1016/j.pgeola.2016.05.003>

Peer reviewed version

License (if available):
CC BY-NC-ND

Link to published version (if available):
[10.1016/j.pgeola.2016.05.003](https://doi.org/10.1016/j.pgeola.2016.05.003)

[Link to publication record in Explore Bristol Research](#)
PDF-document

This is the author accepted manuscript (AAM). The final published version (version of record) is available online via Elsevier at <http://www.sciencedirect.com/science/article/pii/S0016787816300578>. Please refer to any applicable terms of use of the publisher.

University of Bristol - Explore Bristol Research

General rights

This document is made available in accordance with publisher policies. Please cite only the published version using the reference above. Full terms of use are available:
<http://www.bristol.ac.uk/red/research-policy/pure/user-guides/ebr-terms/>

**The Rhaetian (Late Triassic) vertebrates of Hampstead Farm Quarry,
Gloucestershire, U.K.**

**Ellen Mears^{a 1*}, Valentina Rossi^{b2*}, Ellen MacDonald^b, Gareth Coleman^b, Thomas G.
Davies^b, Caterine Arias-Riesgo^b, Claudia Hildebrandt^b, Heather Thiel^b, Chris
Duffin^{b,c,d}, David I. Whiteside^b, and Michael J. Benton^b**

^a School of Earth and Environment, University of Leeds, Maths/Earth and Environment
Building, Leeds, LS2 9JT, UK

^b School of Earth Sciences, University of Bristol, Wills Memorial Building, Queens Road,
Bristol, BS8 1RJ, UK

^c Palaeontology Section, Earth Science Department, The Natural History Museum, Cromwell
Road, London, SW7 5BD, UK.

^d 146, Church Hill Road, Sutton, Surrey SM3 8NF

¹ Current address: School of Geosciences, University of Edinburgh, Grant Institute, James
Hutton Road, Edinburgh, EH9 3FE, UK

² Current address: School of Biological, Earth and Environmental Sciences, Distillery Fields,
North Mall, University College Cork, Cork, Ireland

* Mears and Rossi are equal first authors.

Abstract

The Rhaetian **marine transgression**, which occurred across Europe in the latest Triassic, 205.5 Ma, famously deposited one or more bone beds. Attention has generally focused on the basal bone bed **alone**, but here we explore this bed, and a stratigraphically higher bone bed at the top of the Westbury Formation, and compare the faunas. The Rhaetian at Hampstead Farm Quarry, Chipping Sodbury, Gloucestershire, UK, has produced more than 26,000 identifiable microvertebrate remains, including teeth and scales of chondrichthyan and osteichthyan fishes, as well as vertebrae of sharks, bony fishes, ichthyosaurs, and plesiosaurs. The higher bone bed ('bed 9') contains more small specimens than the basal bone bed, and they are also less abraded, suggesting less transport. Both bone beds yield largely the same taxa, but *Rhomphaiodon minor* and rare *Vallisia coppi* and *Sargodon tomicus* are found only in the basal bone bed. *Duffinselache* is reported only from units above the basal bone bed, but low in the Westbury Formation, and durophagous teeth only from two horizons. Four out of nine chondrichthyan species are common to both bone beds, whereas *Rhomphaiodon minor* and *Ceratodus* are absent, and hybodonts in general are rarer, in bed 9. Bed 9 is the richer source of marine reptile remains, including ichthyosaur teeth, jaw fragments, **vertebrae, rare** plesiosaur teeth and vertebrae, and a few *Pachystropheus* vertebrae and limb bones. Whereas the basal bone bed represents considerable transport and possible storm bed deposition associated with the onset of the Rhaetian Transgression, bed 9 was deposited under **a lower energy regime**.

Keywords: Late Triassic; Chondrichthyes; Actinopterygii; **Marine reptiles**; Bristol; Rhaetian; Rhaetian bone bed; Westbury Formation

1. Introduction

The Rhaetian was an important time in Earth history and in the evolution of life, **leading up** to the end-Triassic mass extinction, ETME (Schoene et al., 2010). After the devastating Permo-Triassic mass extinction, life recovered stepwise (Chen and Benton, 2012), with the appearance of major new groups both in the sea and on land, many of them characteristic of modern ecosystems. For example, on land, while dinosaurs were rising in importance, the precursors of many modern tetrapod groups had emerged, including the first lissamphibians (frogs and salamanders), turtles, lepidosaurs (basal rhynchocephalians), crocodylomorphs, and mammals (Sues and Fraser, 2010; Benton et al., 2014). On land, the ETME was an important trigger in the evolution of dinosaurs, marking the end of the large carnivorous phytosaurs, ornithosuchids, and rauisuchians, and enabling dinosaurs to expand to fill those niches (Brusatte et al., 2010; Benton et al., 2014). The other main terrestrial tetrapod clades, including **crocodylomorphs**, lepidosaurs, and mammals also diversified to some extent after the **ETME**. In the seas, there were major extinctions and turnovers among sharks (Cappetta, 1987, 2012) and marine reptiles (Thorne et al., 2011), whereas bony fishes were apparently unaffected by the **ETME**, with all families passing into the Jurassic (Friedman and Sallan, 2012). Many details of the ETME are still much debated, not least the timing, duration, and magnitude of the event (e.g. Tanner et al., 2004; Mander et al. 2008; Deenen et al. 2010).

The Rhaetian as a stratigraphic stage has also had a chequered history, and its duration is currently debated, with estimates ranging from 7–8 Myr (Muttoni et al., 2010) to 4.4 Myr (Maron et al., 2015). In central Europe and the United Kingdom, the beginning of the Rhaetian is marked by the Rhaetian Transgression, dated at 205.7 Ma (Maron et al., 2015), when marine waters and sediments flooded over the underlying **Mercia Mudstone Group**. In Britain, **the Mercia Mudstone Group red beds pass up into the Blue Anchor Formation, and**

these are overlain conformably, but with a very clear eroded surface, by black and dark grey, bedded marine beds of the Penarth Group, comprising the Westbury Formation and the overlying Lilstock Formation. There is a famous basal bone bed at the base of the Westbury Formation, although it is occasionally absent, and this may comprise microscopic, minimally abraded teeth, scales and bones in some localities, and large-sized abraded blocks of bone, mixed with phosphatized coprolites and inorganic nodules in others (Storrs, 1994; Swift and Martill, 1999; Suan et al., 2012). In places, the base of the Rhaetian is marked by abundant *Thalassinoides* burrows that penetrate the semi-consolidated sediments of the Blue Anchor Formation, and may be filled with gravity-borne bone bed sediments, which were even reworked and packed by the arthropods that produced the burrows (Korneisel et al., 2015). In most places, there may be one or more younger bone beds in the Westbury Formation, generally one, and sometimes several (Duffin, 1980; Swift and Martill, 1999).

The Rhaetian bone beds in England have been sampled at many localities along the outcrop of the Westbury Formation, from Devon in the south, through the Bristol area and South Wales, and across the Midlands of England (Swift and Martill, 1999), and these have been sampled in detail and reported especially from the southern end of the outcrop, around Bristol and Devon (Korneisel et al., 2015; Nordén et al., 2015; Allard et al., 2015; Lakin et al., 2016). Our aim here is to explore a rich locality, Hampstead Farm Quarry, near Chipping Sodbury, south Gloucestershire, in southwest England. The study is based on a unique and extensive fossil collection that was made over many years by Mike Curtis, a renowned local collector, and it is combined with fieldwork, logging, and sampling throughout the Westbury Formation. This allows us to provide one of the most extensive accounts to date of a classic Rhaetian-age marine microvertebrate locality, and to compare the basal and higher bone beds.

Institutional abbreviations: BRSUG, Bristol University, School of Earth Sciences Collection; BRSMG, Bristol City Museum and Art Gallery, Geology Collection.

2. Geological setting

Hampstead Farm Quarry (HFQ; grid reference: ST 726840) is one of a series of quarries, north of Chipping Sodbury, Gloucestershire, UK (Fig. 1). Quarrying began in the area in the Middle Ages, and was intensified in the nineteenth century. From 1844, men in the workhouse were conscripted to break stones for road building, and limestone was also burned in limekilns. When the direct railway route was built from Swindon to South Wales in 1903, a tunnel 4 km long had to be created at Chipping Sodbury, and this brought a railway connection close enough for quarried limestone to be carted down the hill, and quarrying then expanded enormously (Lakin et al., 2016).

Several quarries were excavated on both sides of the Wickwar Road, the B4060, that runs north from Chipping Sodbury, and these are now elongate pits, named Barnhill and Southfield quarries on the west side, and Hampstead Farm Quarry on the east side (Fig. 2). Initially, all the quarrying was close to Chipping Sodbury itself, and in 1929 three separate principal quarries (formerly called Arnolds, Limeridge, and Wilson and Turners quarries, from south to north) were amalgamated into the single, large Barnhill Quarry (ST725830), operated by the new British Quarrying Company, later ARC and now Hanson Aggregates. Barnhill Quarry is no longer worked, and Southfield Quarry (ST723842) houses the offices and rock crushing equipment of Hanson. In 1975, a tunnel was blasted beneath the B4060 road from Southfield Quarry, enabling quarrying to begin on the east side, and so HFQ was created, and it is still actively quarried. Blasted limestone blocks are trucked under the road, crushed and sold for local building and motorway construction.

Hampstead Farm Quarry (Fig. 1) cuts through the overlying Triassic and Jurassic strata to expose older rock units, including the latest Devonian to earliest Carboniferous Tintern Sandstone Formation in the north-east of the quarry, and the Black Rock Limestone, Gully

Oolite, and Clifton Down Mudstone formations (divisions of the Early Carboniferous limestones) successively to the west (Murray and Wright, 1971). These Devonian and Carboniferous beds were folded during the Variscan orogeny, and this imposed the present dip of the Carboniferous beds of 35° to 40° to the west. Numerous thrust faults extend through the Carboniferous beds, which were presumably also formed during the Variscan orogeny (Reynolds, 1938).

At HFQ, the Carboniferous Limestone units are overlain unconformably by the horizontally bedded Rhaetian (Fig. 3a, d). The Rhaetian outcrop at Chipping Sodbury was first recognised by Reynolds and Vaughan (1904), who reported on the sections made available by the railway tunnel and cuttings (around ST728816). In the early days of quarrying in the Barnhill quarries, the Rhaetian overburden was removed to make banks around the quarry perimeter. During excavations eastwards from Southfield Quarry in 1975, to prepare the ground for the new HFQ, a previously unseen section of the Rhaetian was exposed overlying the Clifton Down Mudstone (Curtis, 1981).

The Carboniferous-Rhaetian unconformity in the Chipping Sodbury quarries is unusual because there are so many different Carboniferous units and they all eroded differently; hence, the Rhaetian, and particularly the basal bone bed, occur sporadically depending on the complexity of the topographic unconformity on the underlying lithologies. For example, in Southfield Quarry, Curtis (1981, p. 31) noted that the Carboniferous units had eroded differentially, with the Lower Cromhall Sandstone forming ‘a prominent ridge projecting approximately 3 m above the general level of the erosion surface’. Behind this, a mudstone bed had been eroded to produce a trough 1 m deep. Sandstone boulders eroded from the ridge had filled the trough and were banked as a scree against the ridge.’ He noted that the bone bed was found in the spaces between these boulders, forming a very coarse conglomerate. Further east along the erosion surface lay some isolated boulders, some with fragments of

bone bed attached. The Clifton Down Mudstone had eroded differentially, matching its alternating beds of limestone and calcareous mudstone, and more thinly laminated bone bed was found in the depressions. At the eastern limit of the exposure, the erosion surface dove steeply beneath the Rhaetian cover, reflecting the softer lithologies of the underlying Lower Limestone Shale. The bone bed again occupied depressions on this eroded surface. These **Southfield** Quarry exposures were subsequently quarried out and can no longer be seen.

Attention then shifted to HFQ, where new exposures were created in 1984 in the southwest corner, when overburden was stripped ahead of aggregate extraction, revealing a continuous section from the Carboniferous/ Rhaetian unconformity up through the Westbury Formation and the Cotham Member of the Lilstock Formation (Fig. 3a–c). Mike Curtis, in unpublished notes, describes the excavation of the site in 1984: ‘Removal of the overburden was effected using earth-moving machinery taking successive layers of the Rhaetian rocks only a few centimetres deep at a time. Suspension of these operations from 1985 until 1986 left a plan section of rocks 16 metres by 30 metres close to the Westbury/ Cotham boundary available for study. Vertical sections were available throughout the quarry until stripping was completed in 1990. Limited exposures of the Rhaetian rocks remain around the southwestern corner of the quarry at the time of writing [1999]. The principal discovery during this phase of exposure has been an ossiferous bed at the top of the Westbury Formation containing a vertebrate fauna significantly different from that of the basal bone bed... Other rare elements in this upper bed include well preserved ostracods..., gastropods, echinoid spines and the first British Rhaetian ammonoid (Donovan et al., 1989).’ The site was in the southwestern corner of HFQ (Figs. 2, 3d), and the fieldwork for **the present** study (2014, 2015) was also completed there.

According to the sedimentary log by Mike Curtis (Fig. 4), the Westbury Formation at HFQ comprises nine beds. Bed 1 is a fine conglomerate containing abundant vertebrate

remains. This is the classic ‘Rhaetian basal bone bed’, commonly seen in Rhaetian sections (Storrs, 1994; Swift and Martill, 1999), but at HFQ seen only where the Rhaetian overlies the Clifton Down Mudstone, and not where the Rhaetian sits directly on limestones of the Black Rock Subgroup or the Gully Oolite, because these units formed positive elements of relief on the eroded top surface of the Carboniferous, as noted by Curtis (1981) in Southfield Quarry. The bone bed comprises a fine conglomerate, where grain size seldom exceeds 15 mm, crowded with disarticulated phosphatised vertebrate remains, and with a calcareous matrix. The bones are nearly all heavily abraded, and they make up 55% by volume of the sediment, a further 20% comprising silt, sand, and pebble-sized quartz.

Beds 2 to 8 (Fig. 4) are composed primarily of black shales with calcareous laminae. These include beds with monospecific accumulations of typical Rhaetian bivalves such as *Rhaetavicula contorta* and *Palaeocardita cloacina*, all preserved as decalcified casts, and usually lying convex side up, suggesting some transport and final deposition under conditions of relatively high flow regime. Occasionally, thin white beds of calcareous sandstone occur, as in bed 4, together with sand lenticles in bed 5, all of which weather to an ochreous yellow colour. The impersistent recrystallized limestone in bed 6 is largely unfossiliferous except for occasional bivalves, *Chlamys valoniensis* and rare burrows on its base, as well as some indeterminate bone fragments. Curtis, in his notes, reports sporadic scales and teeth throughout beds 2-8, and a concentration of vertebrate remains in a scour within bed 4, comprising pebbles and clasts of reworked basal bone bed. Small sand-filled channels, measuring up to 30 mm x 100 mm, showed fine, sand-sized vertebrate debris in their bases.

Bed 9 is the uppermost bed in the Westbury Formation at HFQ (Fig. 4). Bed 9 is a 300-mm thick mudstone bed of a black-grey colour that contains a small sandy component, including clasts up to 80 mm in diameter, primarily consisting of weathered limestone intraclasts. The top of bed 9 has a concentration of vertebrate and invertebrate fossils,

including fish teeth and scales, ostracods, echinoid spines, and calcareous shell debris, with fragments of bivalves and gastropods. It is this level that Mike Curtis was able to collect in earnest, and he reported that most of the fossils were ‘fragmentary due to the use of heavy earth-moving machinery for stripping operations. These remains were often discordant with bedding and lay in unstable orientations. For instance, a bone 350 mm in length was found lying at about 30° to bedding, and ichthyosaur vertebrae were found lying on their lateral surfaces. The state of preservation of the vertebrate remains is exceptionally good but many had a buff matrix adhering to them that was lighter than the enclosing sediment. With only one exception, all the vertebrate material in both beds 1 and 9 was disarticulated. The exception was the discovery of several short lengths of euselachian vertebral column containing up to four vertebrae in bed 9.’

Above this (Fig. 4) is the transition to the Cotham Member of the Lilstock Formation, which was up to 3 m thick and comprises buff calcareous mudstones with impersistent buff lenticular limestones. A complete section of the Cotham Member was never exposed during stripping operations. The Westbury/ Cotham junction occurs over a thickness of a few centimetres, comprising alternations of buff and grey laminae, each about 2 mm thick. Fossils are rare in the Cotham Formation, with occasional *Chlamys valonensis* in the basal beds, and teeth and scales of *Gyrolepis alberti* relatively abundant at the base, but diminishing in frequency upwards.

Regional stratigraphy confirms the assignment of the bone-bearing succession to the Westbury Formation of the Penarth Group, a widely exposed and well known unit across southwest England and south Wales (Storrs, 1994; Swift and Martill, 1999). This is amply confirmed by the ostracods, shelly fossils, and vertebrate remains, all of which are typical of the lower Rhaetian. In particular, the ostracods *Ektyphocythere cookiana* and *Ogmoconchella martini*, identified by Boomer (1991a, b) from bed 9 at HFQ, were established as typical of

the uppermost Westbury Formation. Further, palynomorph studies on the same nine beds within the same exposure at HFQ confirm its position within the Westbury Formation and thus its Rhaetian age (Whiteside and Marshall, 2008).

3. Materials and methods

The fossils presented here came from two sources, first, the extensive collection of HFQ fossils made by Mike and Sharon Curtis, now conserved in the BRSMG and BRSUG, and second, the materials from a new excavation in the southwest side of HFQ made during the summers of 2014 and 2015.

3.1. Mike Curtis and the Hampstead Farm Quarry microvertebrate collections

Mike Curtis (1950-2008) was born in Dursley, south Gloucestershire, and he worked as a quarry manager, a bus driver, and then a publican. He and his wife Sharon collected actively throughout the Bristol and south Gloucestershire areas, focusing especially on Rhaetian microvertebrates, and his discoveries include the 1975 finds of *Thecodontosaurus* at Tytherington Quarry (Benton et al., 2012). While he was manager at the Chipping Sodbury quarries in the 1980s and 1990s, he made detailed geological studies of the site, some of which were published (Curtis, 1981; Donovan et al., 1989), but much was left in note form and as unpublished manuscripts dating from 1995, 1999, and 2008. Curtis was able to collect huge amounts of fossiliferous sediment, which he took home and processed by soaking in water and dilute acetic acid, and picking over the residue. His collecting techniques were meticulous; he recorded exact details of the successions of sieves he used and the fossils found at each size level, and he packed the fossils in well-curated boxes and microscope slides with wells, with full details of locality, date and identity. He consulted published accounts and practicing palaeontologists to ensure his identifications were as accurate as

possible. Mike Curtis did not publish on the microvertebrates from HFQ, but he did report the Carboniferous–Rhaetian unconformity at HFQ (Curtis, 1981), as well as a most unexpected discovery, an example of the ammonite *Psiloceras* (Donovan et al., 1989).

The enormous collections amassed by Mike Curtis at HFQ form the basis of this paper. He had donated one large part of his collection to the BRSMG in 1995, and the other half came to the BRSUG after his death, in 2009. The BRSMG collection comprises many thousand specimens, mainly from bed 9, together with ‘a representative collection from the basal bone bed’, stored in 171 boxes and slides. Together with the BRSUG collection, we document nearly 24,000 Curtis specimens from HFQ.

The fossils include vertebrates, invertebrates, and plants. Non-vertebrate fossils include bivalves, ostracods, echinoids, occasional pieces of carbonised wood, and the single ammonite *Psiloceras* (Donovan et al., 1989). Vertebrate remains include teeth, fish gill rakers, fish scales, and occasional bones and bone fragments. They are typically disarticulated, with only one example of articulated elements, but are well preserved with little abrasion or fragmentation.

3.2. Excavated section through the Westbury Formation

A vertical section was dug through the Westbury Formation in the southwest corner of HFQ during summer 2014, and re-examined in summer 2015 (Figs. 2, 4). The section sits unconformably on the Carboniferous Limestone. Twenty rock samples, each weighing about 1 kg, were taken every 20 cm through the section, providing the basis for the description of sediments, and were also processed for their microvertebrate content.

From the bottom of the section, there are 40 cm of pale grey siltstones containing some quartz grains and bivalve shell fragments. Above this are 40 cm of unconsolidated,

homogenous pale grey clays with thin buff-coloured laminae. The first metre ends with 20 cm of medium-grey, laminated siltstone, with some iron content.

The second metre begins with 20 cm of relatively well consolidated, dark grey siltstone with subhedral, colourless quartz grains, about 1 mm in diameter comprising the largest grains in the sample. This sample is generally homogenous, with no lamination. Above this is 40 cm of homogenous, dark grey, unconsolidated siltstones. Above, is a layer of fissile, black siltstone, in which are mm-scale laminations parallel to the bedding. The succeeding 40 cm are characterised by muddy, oxidized siltstone, followed by 20 cm of medium grey fine silt with discrete patches of iron staining. There are cm-scale blocks of well-laminated calcareous silts; the muddy matrix is generally homogenous. The level above consists of fine-grained, homogenous clay, still with some iron staining, and the same colour as the previous units. The third metre ends with 40 cm of homogenous, dark grey silt matrix with abundant laminated, silty, calcareous nodules.

The final metre of the section consists of 20 cm of light grey siltstone, generally homogenous and iron-rich, and then 20 cm of buff-coloured, moderately well sorted silt, less fissile and more consolidated than the previous. Above are 20 cm of medium grey coloured, laminated, homogenous silts, slightly darker than the lower level. These are fairly consolidated, but very easily deformed. Then follows 20 cm of pale grey, quartz-rich silt, rich in angular shell fragments and with blocky texture. Finally, there are 20 cm of pliable, buff-coloured silts, with fine laminations in which was found a cm-scale bivalve fragment. The ubiquitous iron oxides probably indicate anoxic conditions during deposition.

3.3. Sample processing and microfossil study

The rock samples from the 2014 logged section were subjected to preliminary acid treatment and sieving. The acid digestion was made with 1.9 l of water in which 3 g of tri-

1 calcium and 5 g of sodium carbonate anhydrous had been dissolved; at least 100 ml of acetic
 2 acid was added, to obtain a buffered 5% acetic acid solution. The rock samples were placed
 3 in plastic buckets, completely covered with the acid solution and left for 24 hours for
 4 digestion, and then neutralised for 48 hours in water before drying. Acid-water cycles were
 5 repeated 8–12 times until the material had broken down.
 6

7 After that, the residue was washed with water through five sieves of grades 2 mm, 850
 8 μm , 500 μm , 180 μm , and 90 μm . The residue from each sieve was dried on filter paper in a
 9 funnel over a small bucket, and when dry, was brushed into storage bags and labelled
 10 according to the source sample and the processing regime. Next, the samples were picked and
 11 microfossil specimens were separated from inorganic debris. The microfossil specimens were
 12 then classified and counted under an optical microscope. Despite their abundance in some
 13 layers, the sediment overall did not yield large numbers of microvertebrate specimens, and
 14 these comprised principally fragmentary, unclassifiable fossil remains. In the samples taken
 15 from the 2 mm and 90 μm sieves, fossils were often absent, while they were more abundant
 16 in the samples from the other sieves. In total, 2508 specimens were extracted and counted
 17 from our 2014–2015 field work.
 18

19 For the older collections, Mike Curtis reported that he treated his samples from bed 1
 20 with 10% acetic acid, whereas those from bed 9 required only to be disaggregated in water.
 21 He then ran the materials through a careful regime of sieving, noting which specimens were
 22 retrieved at different sieve sizes, namely of 2.4 mm, 1.2 mm, 600 μm , and 300 μm gauge. His
 23 methods are outlined further by Korneisel et al. (2015).
 24

25 BRSUG and BRSMG numbers are used throughout. Where there are multiple
 26 specimens on a single slide, those that are described or illustrated are labelled with additional
 27 numbers and letters, describing the position in terms of rows (e.g. row 1, 2, 3, etc.) and
 28 columns (e.g. column a, b, c, etc.). With multiple specimens in a box bearing a single
 29
 30
 31
 32
 33
 34
 35
 36
 37
 38
 39
 40
 41
 42
 43
 44
 45
 46
 47
 48
 49
 50
 51
 52
 53
 54
 55
 56
 57
 58
 59
 60
 61
 62
 63
 64
 65

1 catalogue number, similarly we identify those that are figured or described with additional
2 letters, so they can be distinguished from the others in the same box.
3

4 The teeth, scales, spines, and other vertebrate fossils were examined under an optical
5 microscope and classified into morphotypes. The fossils were measured using the in-built
6 eyepiece graticule (accurate to 0.1 mm). While the height and width ranges for different
7 morphotypes are provided in the descriptions below, the fossils are typically incomplete, and
8 so any measurement is likely to be an underestimate of the actual size. In the descriptions of
9 teeth, 'height' refers to the distance from the apex of the crown to the bottom surface of the
10 root (where both are present), while 'width' was measured as the widest part of the tooth.
11 Both measurements were made with the base in a horizontal position. In multicusped
12 chondrichthyan teeth, height is measured at the tallest cusp.
13
14
15
16
17
18
19
20
21
22
23
24
25
26

27 The best example of each morphotype was photographed using a Leica DFC425 C
28 camera supported by an optical microscope. The intuitive progressive scan preview in XGA
29 resolution was used, and it provided up to 20 frames per second (fps) and allowed the sample
30 to be adjusted and focussed directly on the computer screen. Thanks to the multi-focus
31 option, it is possible to have images in perfect focus, even when the photographed object is
32 not perfectly flat, as is the case with teeth or bones. A scale was included in each photograph,
33 and these were processed using Adobe Photoshop© to remove backgrounds and improve the
34 contrast and colour balance before being compiled into multi-element figures.
35
36
37
38
39
40
41
42
43
44
45
46
47
48
49
50

51 *3.4. Identification of specimens and faunal composition*

52 Where possible, taxa were identified using available literature. Any specimens that could not
53 be identified were assigned to numbered morphotypes, but a preliminary identification as
54 chondrichthyan, osteichthyan, or reptile was usually possible. Once classified, numbers of
55 specimens were counted. However, several issues were encountered. First, while most
56
57
58
59
60
61
62
63
64
65

specimens were single teeth, a few were composed of several teeth articulated together.

Solely counting either each tooth or each specimen (i.e. counting a specimen of several fused teeth as one) would result in bias; many of the individual teeth may have come from a single individual, like the articulated teeth, but this cannot be confirmed for isolated teeth. It was decided, following Van den Berg et al. (2012), that both forms of counting would be included in analyses of the faunal composition. In addition, many fish display heterodonty, and several of the unclassified morphotypes may be from the same species, and so some species numbers may be overestimated. Where identified species are known to be heterodonts, all forms are classified as a single morphotype.

4. Systematic palaeontology

In this section, we review all the micro- and macrovertebrate specimens, separating the remains of fishes from reptiles. We identify named taxa only where supported by previous research, and many remain, unfortunately, as unnamed morphotypes, as is normal practice in such work.

4.1. Chondrichthyan teeth

Seven tooth types are assigned to named chondrichthyan taxa, all common forms in the British Rhaetian. There are additional chondrichthyan dermal denticles/ scales that have not been studied in detail.

4.1.1. *Duffinselache holwellensis* (Duffin, 1998b)

Duffinselache holwellensis teeth are wide mesiodistally, with a single, distally inclined, shallow central cusp, but no lateral cusplets (Fig. 5a–c). The cusp has a diamond-shaped basal cross section. The teeth vary from being almost symmetrical in examples from anterior

parts of the dentition (Fig. 5a–b), to asymmetrical in specimens from more posterolateral positions (Fig. 5c). The mesial and distal heels of the crown extend laterally from the central cusp, and are ornamented by strong vertical non-branching ridges. These ridges are largely confined to the crown shoulders in symmetrical teeth (Fig. 5a–b), but descend from the rather weak occlusal crest in asymmetrical specimens (Fig. 5c). In some specimens, this ornamentation is very worn. A strong neck separates the crown from the root. The root itself is approximately the same depth as the crown, which it underlies directly in symmetrical teeth, and from which it is slightly offset **lingually** in asymmetrical examples. Vertically accentuated vascular **foramina** punctuate the labial surface of the root at regular intervals, and are separated by columns of intervening root tissue. **Foramina** entering the lingual face of the root do so almost horizontally (Fig. 5c). Some specimens have slight tubercles on the lateral heels of the crown.

These teeth clearly belong to *Duffinselache*, a monotypic genus first described from a fissure infill of Rhaetian age from Holwell in Somerset, and also from a bone bed within the Westbury Formation black shales at Chilcompton in Somerset (Duffin, 1998b, 1999). This is confirmed by the slim, elongate shape of the crown combined with the single cusp, simple crown ornament of unbranched vertical ridges, and root architecture. Originally placed in the hybodonts as a species of *Polyacrodus*, subsequent examination of the ultrastructural histology of the crown indicated that the species is a neoselachian shark, based on the presence of a distinctive triple-layered enameloid (Andreev and Cuny, 2012).

4.1.2. *Lissodus minimus* (Agassiz, 1839)

Lissodus minimus teeth have a boomerang-shaped crown (Fig. 5d–f). There is a single low, upright central **cusp, ornamented** by a radiating system of frequently bifurcating vertical ridges descending the crown from the cusp apex and the strong occlusal crest on the lateral

heels of the crown (Fig. 5e). Up to five pairs of very low lateral cusplets may also be present, flanking the central cusp. A horizontal ridge may be developed around the tooth at the crown shoulder, especially in larger specimens (Fig. 5e). Typically, there is a globular projection, the labial peg, at the base of the crown on the labial side of the tooth, and this may possess a contact scar where it abuts against the lingual surface of the succeeding tooth in the revolver (Fig. 5d). Most specimens are very worn, and roots are rarely attached (e.g. Fig 5d). When present, the root is at least the same depth as the crown, with a labiolingually flattened basal surface that is arched in labial view (Fig. 5f). Each surface of the root is punctuated by numerous randomly distributed vascular foramina; a row of small circular foramina is commonly present just beneath the crown/root junction labially, giving way to a system of much larger foramina centrally and further small circular foramina basally (Fig. 5f).

Originally allocated to *Acrodus* by Agassiz, teeth of this species were transferred to *Lissodus* when the latter genus was reviewed by Duffin (1985, 2001).

4.1.3. *Pseudocetorhinus pickfordi* Duffin, 1998a

The teeth of *Pseudocetorhinus pickfordi* (Fig. 5g-m) have an opaque crown with a thorn-like single, pointed cusp that may be inclined both distally and lingually (Fig. 5g and h). The teeth measure up to 0.5 mm long (mesiodistally) and 4.5 mm high at the central cusp. The cusp is typically situated at the midpoint of the tooth, but may be slightly offset distally (Fig. 5i and j); typically, no lateral cusplets are developed, although incipient lateral cusplets have been noted in a few specimens. The crown is unornamented. The crown/root junction is rather more strongly incised labially than lingually. The root itself is approximately the same height as the crown and has a strongly corrugated, rugose surface.

Teeth from presumed anterior and anterolateral positions on the jaw are robust with a relatively upright central cusp and show varying degrees of asymmetry (Fig. 5g, h, k, l). The

mesial heel of the crown is longer than the distal heel. A moderate cutting edge formed by the occlusal crest runs the length of the crown mesiodistally, passing through the central cusp apex. The root projects lingually from the crown underside. The mesial and distal lobes of the root extend well beyond the mesial and distal heels of the crown. The basal face of the root is relatively flat overall, but strongly arched in labial and lingual views (Fig. 5g, k).

In presumed posterolateral teeth, the crown is much lower; the central cusp is considerably reduced in height and more distally and less lingually inclined than in anterolateral teeth (Fig. 5i). The tooth itself is also less robust. The root more directly underlies the crown, the basal face is not arched, and the lateral lobes of the root do not project beyond the lateral heels of the crown (Fig. 5i and j).

An unusual tooth, clearly belonging to *Pseudocetorhinus pickfordi* is illustrated in Figure 5m. Upright with the root directly underlying the crown, the tooth is small and higher (1.1–2.2 mm) than it is mesiodistally (1.0–1.5 mm). The central cusp is very low, acorn-shaped, laterally compressed and pointed. The cutting edge is weakly developed and two vertical ridges descend the crown from the cusp apex, one labially and one lingually. There are also other faint, incipient ridges on the crown. The lateral heels of the crown are draped over the surface of the root mesially and distally. A moderate neck separates the crown from the root. The root comprises two-thirds of the total tooth height, and flares at its base. It is unclear from which part of the dentition this tooth is derived.

Curtis originally classified five specimens as being ‘*Hybodus* sp. nov.’ in his notes; these specimens plainly belong to *P. pickfordi* (Fig. 5k and l).

Duffin (1998, 1999) also described some gill raker teeth which he associated with *Pseudocetorhinus pickfordi*, assuming that the species was a filter feeder, and following comparison with extant filter-feeding sharks. Curtis’s collection from HFQ contains numerous examples of similar gill raker teeth, which, because they are very delicate, are rare

in other Rhaetian deposits. The teeth are 5 mm long, elongate and laterally compressed with a flared base. They narrow toward a sharply pointed translucent tip (Fig. 5n). In the summary counts of fossils below, we combine these gill raker teeth with the *Pseudocetorhinus* teeth.

4.1.4. *Synechodus rhaeticus* (Duffin, 1982)

Teeth of *Synechodus rhaeticus* are usually complete (Fig. 6a–h) and measure up to 4 mm mesiodistally and 2 mm high at the central cusp. Anterior and anterolateral teeth are relatively symmetrical (Fig. 6a–d), possessing a high, upright to slightly distally and lingually inclined central cusp, sometimes positioned slightly off-centre, flanked by an average of three smaller lateral cusplets on each side (Fig. 6a–d). The height of the lateral cusplets decreases away from the central cusp. In posterolateral teeth, the crown has a much lower profile, with a short central cusp flanked by up to five pairs of low lateral cusplets (Fig. 6e–h). The crown is ornamented with strong vertical ridges that descend both the labial and lingual faces of the crown from the cusp apices. At the base of the crown, the ridges branch and anastomose, producing a reticulate pattern that extends over the crown shoulder for the full length of the tooth, but is more extensively developed labially (Fig. 6c–h). The crown/root is deeply incised, but the lateral lobes of the root do not extend beyond the mesial and distal heels of the crown. The root is punctuated by numerous foramina. The root is more arched in anterior and anterolateral teeth than it is in posterolaterals (compare Fig. 6b and 6f).

These distinctive teeth clearly belong to *S. rhaeticus*, a species recorded from the Rhaetian of Britain and continental Europe (Duffin, 1998b, 1999; Cuny et al., 2000).

4.1.5. *Polyacrodus cloacinus* Quenstedt, 1858

Specimens of *Polyacrodus cloacinus* consist of isolated multicuspid crowns that are elongate mesiodistally (Fig. 6i and j). The central cusp is tall and flared at the base. It is

flanked by up to six pairs of **inclined** lateral cusplets that diminish in **height away** from the central **cuspl**. The surface of the crown has strong vertical ridges, **descending** both labially and lingually from the cusp apex, bifurcating basally in some specimens. The vertical ridges are coarser on the labial face of the crown **than on** the lingual face. The vertical ridges may cross the crown shoulder and terminate just above the crown/root junction. A distinctive labial node is developed **towards** the base of the central cusp. The teeth are asymmetrical, with rather more mesial lateral cusplets than distal ones (6 mesial cusplets and 1 distal in Fig. 6i and j). None of the specimens is intact, and none has a preserved root.

The combination of a relatively narrow central cusp and lateral cusplets, together with the presence of strongly developed labial nodes distinguishes *P. cloacinus* from all other Late Triassic and Early Jurassic large hybodont teeth (Duffin, 1993).

4.1.6. *Vallisia coppi* Duffin, 1982

Vallisia coppi teeth are small (1.5 mm high) with three upright to slightly inclined cusps that are flattened labio-lingually (Fig. 6k), and have confluent bases **forming** the remainder of the crown basally. The central cusp is the tallest of the three. The surface of the crown is unornamented. The base of crown is expanded to overhang the root; the crown/root junction is very deeply incised. The base of the root is flared and has two lateral lobes flanking a medial canal.

These highly distinctive teeth have also been described from the Rhaetian of Vallis and Holwell, both in Somerset (Duffin, 1982), Manor Farm Quarry (Allard et al., 2015) and Belgium (Duffin et al., 1983). The most recent taxonomic consideration of *V. coppi* places it in the *Neoselachii incertae sedis* (Cappetta, 2012, p. 327).

4.1.7. *Rhomphaiodon minor* (Agassiz, 1837)

These teeth are high-crowned, measuring just over 1 mm tall, with a triangular, symmetrical central cusp (Fig. 6l and m). The cusp is sharply pointed and flanked by one or two pairs of lateral cusplets, measuring about a quarter of the height of the central cusp, all of which are lingually inclined. Both labial and lingual faces of the crown are ornamented with a series of coarse vertical ridges that descend from the cusp apices, occasionally bifurcating basally, and terminating just above the crown/root junction. The cutting edges of the cusps are moderately sharp. The root is shallow, generally forming around one third to one quarter of the total tooth height, and projects lingually from the crown underside, developing into the so-called lingual torus (Fig. 6l).

Teeth of this species were associated with the dorsal fin spine described as *Hybodus minor* by Agassiz (1837 in Agassiz 1833-1844). Long believed to belong to a hybodont shark, teeth of this type have subsequently been allocated to the neoselachian shark *Rhomphaiodon*, on the basis of their morphology and enameloid ultrastructure (Cuny and Risnes, 2005).

4.2. Osteichthyan teeth

Four distinct osteichthyan tooth genera are identified, all of them common forms in the British and European Rhaetian.

4.2.1. *Gyrolepis albertii* Agassiz, 1835

Gyrolepis albertii is represented by conical teeth composed of a translucent acrodin tip and a shaft with a slightly flared base (Fig. 7a and b). Long specimens typically have inclined shafts, although the acrodin tip is always straight and conical, and unornamented. The remainder of the crown is usually smooth, although it can be moderately ridged.

Gyrolepis albertii was originally named for specimens from the Muschelkalk (Middle Triassic) of Germany and the Rhaetian of Wickwar (Gloucestershire) by Agassiz (1835 in Agassiz 1833-1844, vol. 2, p. 173). Seemingly a taxon with rather a wide stratigraphic range, *Gyrolepis albertii* is in considerable need of review.

4.2.2. *Severnichthys acuminatus* (Agassiz, 1835)

Two tooth shapes are identified as belonging to *Severnichthys acuminatus*, which were originally classified as separate taxa (*Birgeria acuminata* and *Saurichthys longidens*). In this paper, both types are classified together as *Severnichthys acuminatus*, following Storrs (1994), although the two morphologies are distinguished here for the purposes of description.

‘*Birgeria*’-type teeth have an overall conical to bladed shape (Fig. 7c and d). The tooth has a transparent acrodin tip ornamented with moderate vertical ridges. The cap may be slightly compressed, presumably in a lateral sense. The lower portion of the tooth is dark brown, with a rugose appearance owing to strong vertical ridges. There is a strong neck separating the two parts of the tooth.

The ‘*Saurichthys*’-type tooth (Fig. 7e) has a small, smooth, conical acrodin tip, which is smaller than those found in the ‘*Birgeria*’-type and is a smaller portion of the tooth as a whole. The neck is less well defined than in the ‘*Birgeria*’ morph, and the lower portion of the tooth has a very rugose surface. Although superficially similar to *Gyrolepis albertii*, the ‘*Saurichthys*’ morph differs by having much stronger ridges on the lower part of the crown, and by being less pointed and less inclined than *G. albertii*.

4.2.3. *Sargodon tomicus* Plieninger, 1847

Sargodon tomicus is also a heterodont species, with two types of teeth, a molariform type and an incisiform type. Both tooth types possess a heavily mineralised acrodin cap

penetrated by **bundles** of dentine tubules (vascular acrodin). The molariform tooth is hemispherical to **rectangular** (Fig. 7f), **and** typically heavily worn, creating a flat apical surface. Only the crown is present in **the** HFQ specimens.

The incisiform teeth are much **taller, and** have a very different morphology with an overall chisel shape (Fig. 7g and h). The crown is relatively short with a pointed apex and a slightly bulbous base. The root is composed of a long, straight cylindrical shaft that flares out at its base.

Originally named by Plieninger (1847) for distinctive teeth from the Rhaetian of Germany, this taxon has since been recorded throughout northwest Europe, and also in the Norian of Italy (Tintori, 1983).

4.2.4. *Lepidotes* sp.

Lepidotes sp. is represented by two specimens, **one with** a central wear facet on the labial side of the tooth, dividing the crown in two (Fig. 7i), and **the** other a globular tooth with no apparent ornamentation (Fig. 7j). In the latter, there is a large tubercle close to the apex of the tooth. The specimen does not appear to have a root. Typical *Lepidotes* teeth from the British Rhaetian are found with attached roots, which constitute two thirds or more of the total height. The root is bulbous and sometimes shows fine striations (Moore, 1867; Richardson, 1911; Sykes, 1979; **Duffin, 1980**; Nordén et al., 2015, p. 574).

4.2.5. *Morphotype O5: Durophagous tooth plate*

A number of small elements bearing multiple teeth have been noted (Fig. 7k). In this case, there are two or three tiny, rounded boss-like teeth per mm. These are very similar to jaw fragments noted by Nordén et al. (2015, fig. 9M and N) from the Marston **Road Rhaetian** bone beds, with smooth, dome-shaped and very worn teeth of different size and numbers.

Tooth plates such as these are typical of durophagous fish, but abrasion and the often very fragmentary state of the plates makes it hard to assign them to a taxon.

4.3. *Neoselachian vertebrae*

A large number of chondrichthyan vertebrae are present, all of which are identified as *Neoselachii*. The origin of the *Neoselachii* is debated. There is a case for suggesting that the earliest neoselachians are known from the Palaeozoic (Duffin and Ward 1993; Ginter et al., 2010), and they diversified substantially during the Late Triassic and the rest of the Mesozoic; these *Rhaetian specimens* are important in documenting the early history of the clade (Cuny and Benton, 1999). Neoselachian vertebrae from HFQ have been classified into three morphotypes based on distinct characters (Fig. 8), but they cannot be assigned to taxa. All show fairly extensive abrasion, more so than the teeth, which are protected by enamel.

4.3.1. *Morphotype V1*

Morphotype V1 (Fig. 8a and b) is roughly cylindrical, with rounded edges and smooth sides. There is slight lateral compression around the sides of the vertebrae, to the extent that some show four distinct faces on the side, much like a cuboid. The tops are mostly smooth and rounded. They range in size from 1–15 mm and comprise 45% of the vertebral collection.

About half the examples of this morphotype are broken, retaining one articular face, because the middle part of the vertebra is weakest and susceptible to post-mortem breakage and wear. In such broken examples, the internal structure comprises concentric rings, which are the eroded layers of calcified tissue that makes up the cyclospondylous centrum. The canal of the constricted notochord is sometimes visible on the eroded surface.

4.3.2. *Morphotype V2*

Morphotype V2 (Fig. 8c and d) is similar to morphotype V1, except that the general shape is somewhat less regular and even. It is roughly cylindrical, with rounded edges. The sides show lateral compression, often to a larger extent than in morphotype V1. The tops also show some slight dipping in the middle. The most obvious distinctive feature is the occurrence of prominent ridges and grooves on the sides, the surface expression of the internal structure, showing that these vertebrae are weakly asterospondylous. These vertebrae range in size from 1–15 mm. This is the second most common morphotype, comprising 37% of the vertebrae.

4.3.3. Morphotype V3

Morphotype V3 is cylindrical, with rounded tops with smooth edges. The tops have a depression in the centre, as in morphotype V2. It also exhibits a large degree of lateral compression, along with some torsion, giving each vertebra a distinct ‘dumbbell’ shape (Fig. 8e and f). The vertebrae range in size from 1–15 mm. This morphotype is the least common, making up just 6% of the vertebrae. These show some resemblance to vertebrae described from the Lower Lias of Lyme Regis as part of articulated specimens of *Synechodus* and *Palidiplospinax* (Duffin and Ward, 1993; Klug and Kriwet, 2008).

4.3.4. Unclassifiable vertebrae

Some of the vertebrae, comprising 12% of the total number, could not be classified. These include fragments of vertebrae, and vertebrae of indeterminate shape and morphology, as well as specimens that are weathered and abraded to the point where they cannot be identified.

4.4. Chondrichthyan denticles

In the HFQ samples, many small denticles have been identified, all deriving from the dermal covering of chondrichthyans. There are a number of placoid denticles of different morphologies, as well as chimaeriform denticles.

Sykes (1974) described chimaeriform denticles as rare in the Westbury Formation. The morphotypes found in HFQ vary in size. All have large, rounded basal plates with radial grooves and a concave underside. The basal plates are thick and make up half the height of the specimen. There is usually one crown. Curtis did not separate these denticles into different morphotypes, but we identify four.

4.4.1. Morphotype D1

This morphotype (Fig. 9a–d) is fairly common. The cap is conical and varies in height and angle. In some specimens the cap is fairly pointed posteriorly and in others the cap is slightly flattened. The width of the cap is about a third of the width of the base and from above appears elliptical, although in some the cap is circular. Generally the shape of the cap mirrors the shape of the base. The height of the base relative to the cap is smaller than in the other two morphotypes. The ridges on the base are radial and point towards the centre of the denticles. These compare closely with denticles of the menaspiform holocephalan *Menaspis armata* (Sykes, 1974).

4.4.2. Morphotype D2

Morphotype D2 (Figure 9e and f) is the least common, with only five specimens identified. This type also has a round to elliptical base, but the cap is angled approximately 45 degrees anteriorly. The cap is very rounded and flattened at the top. The base is tall and narrows quickly towards the cap. The striations on the base are radial but point towards the cap and the anterior side of the denticles.

4.4.3. Morphotype D3

Morphotype D3 (Fig. 9g and h) shows the most variation, but all specimens share the following traits. The base is thick compared to the height of the denticle and the underside is much less concave than in the other types. The cap is angled anteriorly in some specimens, but generally the surfaces of the caps are still fairly flat. The caps have ridges along the posterior edge that are usually symmetrical, but not radial, creating an arrow-head shape from above. Some of the specimens do not have such an obvious arrow shape, but can still be identified by the steep, straight edges of the cap.

4.4.4. Morphotype D4

Morphotype D4 (Fig. 9i and j) is distinctive. The crown has a long, thin, cylindrical process that is slightly compressed laterally, and narrows from the neck towards the apex, and is inclined posteriorly. The flared, polygonal base is strongly ridged radially, and these ridges run to the margins of the base, producing a feathered edge. Where the base is not intact, the foramina are exposed. Specimens measure 2.0 mm high and 1.2–1.8 mm wide. Denticles of this morphotype most strongly resemble the dermal structures described from the revetment of scales found on the ventral margin of the frontal clasper in male specimens of *Squaloraja*, and in the opposing skin of the ethmoid region of the skull (Delsate et al., 2002, p. 24; Duffin, 2010, p. 340, fig. 31).

4.4.5. Placoid denticles

The HFQ placoid denticles range in size from 250 μ m to 1.5 mm. Altogether, 349 specimens were identified, and these fall into four morphotype groups based on the shape of the basal plate and crown. Morphotype A (Fig. 9k) has a square basal plate with a crown of

equal geometry. Lateral keels are not observed to reach the tip of the crown, so creating a flat-topped square crown. Morphotype B has a hexagonal basal plate with a crown of equal geometry; the crown reaches a height of 1 mm and the basal plate is up to 2 mm in length. Like Morphotype A, the lateral keels do not reach to the crown, resulting in a flat-topped crown surface. Morphotype C also shows similar shapes of the crown and basal plate, but the shapes include equilateral triangles (often with the apex of the triangle missing), tear drops and arrowheads. Morphotype D shows a winged or bladed crown geometry sitting on a rounded to square basal plate.

4.5. *Osteichthyan scales*

The abundant osteichthyan scales from HFQ are all rhomboid, but vary in shape from almost square to parallelograms (Fig. 10). The scales are covered by a thin layer of ganoine, which is finely striated in some specimens. Ganoid scales are found today only in chondrosteans such as bichirs and reedfishes (Family Polypteridae) and holosteans such as gars (Family Lepisosteidae). The scales do not overlap, but have complementary ridges and chamfered edges to accommodate neighbouring scales. Some of the morphotypes possess pegs on the anterior-ventral side and corresponding notches on the underside of the scale, locking together in life.

4.5.1. *Gyrolepis albertii* Agassiz, 1835

These scales are the most common, comprising almost 75% of identifiable scales in bed 9; they are generally the most frequent scales in British Rhaetian bone beds (Storrs, 1994, fig. 5A). The scales are rhomboids but are extended in the anterodorsal to posteroventral direction to give a somewhat sigmoidal outline (Fig. 10a and b). A thick layer of ganoine covers the scale apart from the anterior portion, which in life is overlapped by the scales

immediately in front. The exposed portion of the scale is striated by ridges in the ganoine, passing diagonally across the scale from the top right corner to the bottom left corner. These striations show slight bifurcation. The reverse of the scale shows a wide vertical ridge. The anterior and dorsal sides are chamfered to fit adjacent scales.

4.5.2. Morphotype S2

These scales are also rhomboidal, but show a much wider anterior portion where the adjacent scale overlaps, and the dorsal edge is rounded (Fig. 10c and d). This morphotype is characterised by two anterior pegs, the upper peg extending from the dorsal edge and the lower peg being slightly thinner than the rest of the scale. The second peg is part of a chamfered edge and the dorsal edge is slightly bevelled. The striations run antero-posteriorly, with some bifurcation towards the central, broader part of the scale. The striations are coarser than in the *Gyrolepis albertii* scales. On the reverse of the scale there is a medial indentation to accommodate the lower peg. These have been interpreted as possibly being dorsal scales of *Gyrolepis albertii* (Sykes, 1979) or scales of *Lepidotes* (Sykes, 1979).

4.5.3. Morphotype S3

This morphotype (Fig. 10e and f) also has a peg and a socket articulation, and scales are rectangular and rhomboidal. The anteroventral edge is curved and acutely bevelled. The dorsal edge has a very broad chamfer to fit under the scale above. Below this chamfered edge is a layer of striated ganoine, with striations oriented anterodorsally to posteroventrally. There are normally about 13 striations and bifurcation is not common. The posterior edge is chamfered. There is a fine lateral ridge that terminates anteriorly. The socket to receive the peg is slightly below the ridge; the offset creates a staggered pattern of scales. The affinities of these scales are uncertain, but they may be specialised scales from *Gyrolepis*.

4.5.4. Morphotype S4

Scales of this morphotype (Fig. 10g and h) are rare, and Curtis identified only six examples from HFQ. The scales are rhomboidal and are almost entirely covered in a thick layer of ganoine, which shows narrow growth rings on the outer surface (Fig. 10g). The ganoine lacks striations but is slightly concave centrally. There is also often a small ridge and crack in the ganoine layer in the anterodorsal corner and the posterior edge can be chamfered. The internal face (Fig. 10h) is featureless apart from its convex shape. These are possibly *Pholidophorus* scales, but these specimens are much larger than would be expected. Note, however, that scales of this size and type, including growth rings, have been reported from the palynologically dated (Rhaetian) fissure 13 at Tytherington, and also assigned to *Pholidophorus* (Whiteside and Marshall, 2008, fig. 5 hh, ii, jj).

4.5.5. Morphotype S5

This type is rare. The scales are the largest of the morphotypes and are square (Fig. 10i and j). A striated ganoine layer covers nearly all the scale apart from the chamfered anterior edge. The striations differ from those in the other scales in being directed diagonally rather than antero-posteriorly, in being more widely spaced, and in bifurcating more regularly and frequently. Characteristic of this morphotype are striations that terminate in crenulations near the dorsal margin. Similar crenulations were also observed in a *Gyrolepis albertii* specimen (BRSMG Csb698-5), and appear to be as a result of weathering.

4.6. Osteichthyan fin ray elements

Some osteichthyan fin ray elements, lepidotrichia, the structures that provide stiffening of the fins, have been identified in the collection. In life, the rod-like lepidotrichia

are embedded in the fin connective tissue, and **comprise** short bony segments, **jointed and** connected by collagen fibres. Each fin ray element comprises a bony core with a ganoine-like outer layer, and they are often found associated with the ganoine-covered scales of *Gyrolepis* and other osteichthyans. Curtis identified four distinct morphotypes among the osteichthyan fin ray elements from HFQ, but they cannot be assigned with certainty to any of the taxa identified **from teeth**.

4.6.1. Morphotype F1

These fin elements (Fig. 11a–d) are plate-like and **sigmoidal, extended** in the anterodorsal to posteroventral direction, but with parallel dorsal and ventral edges. The anterior and posterior edges are **curved, and they are** chamfered to accommodate adjacent elements. A thin layer of striated ganoine is present near the anterior **margin**. Larger specimens (Fig. 11c and d) are extended in the dorsoventral direction and **are sigmoidal**.

4.6.2. Morphotype F2

This fin ray element morphotype (Fig. 11e and f) is squat with a square base. There is a steep ridge on the front of the element, creating a **domed cross section**. A layer of striated ganoine covers up to 50% of the **element**. A chamfered protrusion on the anterior **margin slots** into a complementary ridge on the **posterior margin**. On the reverse side there is a deep indentation and the posterior edge is chamfered to accommodate the next element.

4.6.3. Morphotype F3

Morphotype F3 (Fig. 11g and h) is very similar to morphotype **F2, but** instead has a crescent-shaped protrusion on the anterior edge. Striated ganoine is present in a thin layer

near the dorsal edge. On the back of the element there is another raised ridge, creating a circular cross section. The posterior edge is chamfered to fit the next element.

4.6.4. Morphotype F4

This **morphotype** (Fig. 11i and j) is thin and elongate compared to the **others**. The element ends in a point on the posterior side. In the **centre**, **ganoine** is present, but in nearly all specimens **it has** been removed **by abrasion**. The reverse of the structure has a thin ridge in the anteroposterior direction with an indentation below. **These** elements might represent **specialised** scales from the tail region of **the fish**.

4.7. Marine reptiles

Reptilian remains are relatively abundant in the Westbury Formation, but most are fragmentary or isolated elements of little taxonomic value (Storrs, 1994). Among the recognizable elements are isolated vertebrae and other fragments of ichthyosaurs and plesiosaurs. Because of the generally conservative nature of the postcranial elements of these marine reptiles, however, they generally cannot be assigned to genera. Other reptile components common in the bone beds of the Westbury Formation are vertebrae and long **bones** of the early choristodere (or thalattosaur) *Pachystropheus rhaeticus* (Storrs, 1994; Swift and Martill, 1999; Allard et al., 2015).

4.7.1. Ichthyosaurs

The ichthyosaurs were highly specialised marine **reptiles**, and **those** from the Penarth Group are generically indeterminate, comprising isolated conical, grooved teeth, disk-like and deeply amphicoelous vertebral centra, ribs, and paddle elements.

4.7.1.1. *Ichthyosaur teeth*

Several ichthyosaur teeth show a wide range of shapes and sizes, corresponding to their natural variations from front to back of the jaws. Smaller specimens measuring 7.2–11.6 mm in height and 4.0–5.2 mm in width appear to preserve only the crown, with no root attached. The surface of the crown is highly ornamented, with curved, branched ridges creating a grooved surface. The teeth are conical, and are upright to inclined. They are slightly compressed, producing two carinae that presumably acted as cutting edges.

The largest ichthyosaur tooth (Fig. 12a and b) also lacks the tip of the crown, but the lower portion of the crown and the root are well preserved. The tooth appears gently curved and laterally compressed, with a total height of 20 mm. The crown and root show folds of dentine (plicidentine), and these folds begin as reasonably regular grooves and ridges in the crown, but expand and become deeper and more irregular on the outer face of the root.

4.7.1.2. *Vertebrae*

Among the collection there are twelve ichthyosaur vertebrae, with centrum diameters ranging from 10–35 mm. The largest are well preserved, although some diagnostic elements are not present, while the smallest are greatly abraded and incomplete. The centra are deeply amphicoelous, and they always lack the small neural arch, which presumably became separated early in the transport process. Ichthyosaurs typically have 100–200 vertebrae, with some shape variation from neck to trunk to tail, and substantial size reduction towards the tip of the tail (Storrs, 1999). Even though isolated vertebrae cannot be identified to genus, they can be assigned to the approximate region of the vertebral column.

We describe three types of vertebrae: an anterior trunk vertebra, a middle trunk vertebra, and an anterior caudal vertebra. The anterior trunk vertebra (Fig. 12c–e) is slightly heart-shaped in articular view, broader than tall, and with a central deep depression on each

articular face. In lateral view (Fig. 12d), the diapophysis and parapophysis may be seen near the anterior edge of the centrum, and in dorsal view (Fig. 12e) the symmetrical ridges form the facets for the neural arch.

Middle trunk vertebrae are larger and longer (Fig. 12f–h). The articular face (Fig. 12f) is taller than in the anterior trunk vertebra, and the overall shape of the articular face is square with rounded corners. The anterior margin in lateral view (Fig. 12g) is bevelled from mid-height ventrally, but the diapophysis and parapophysis cannot be distinguished. The neural arch facets are deeply incised (Fig. 12h).

The anterior caudal vertebra (Fig. 12i–k) is again smaller and thinner and with polygonal articular faces. The rib attachment is clear in lateral view (Fig. 12j).

4.7.1.3. Scapula

The scapula (Fig. 13a and b) is incomplete, and consists of the expanded proximal end with the base of the narrow elongated scapular blade. The anterior margin of the element is straight and thin, and curves around the anteroventral acromion process into the ventral, straight coracoidal contact. On the posterior margin, this contact flares and thickens to form the upper portion of the glenoid facet for insertion of the humerus. The scapular blade is narrow and would have extended in life as a straight-sided element. The orientation of acromion process and glenoid indicate that this is a right scapula.

4.7.1.4. Femur

There is one nearly complete ichthyosaur femur (Fig. 13c–e), although the proximal end is abraded. The proximal epiphysis is absent, but the remainder shows the classic shape (e.g. Lomax and Massare, 2015), with a 90° twist of the shaft, and the flattened and widely expanded distal end, with two broad articular surfaces for the tibia and fibula. The articular

surface appears irregularly pitted, showing that cartilage intervened between the propodial and epipodials. This is presumably a right femur because the longer tibial facet is located anteriorly.

4.7.1.5. Paddle bones

It is difficult to identify the epipodial and autopodial elements of ichthyosaur paddles when the fossils are disarticulated and isolated. In the collection there are 14 paddle elements, ranging from 5–30 mm in diameter, and it is impossible to determine whether they come from fore or hind paddles. Among these elements are circular and polygonal elements (Fig. 13f–i). Most of these are fragmented and abraded.

4.7.2. Plesiosaurs

Plesiosaur bones are less common in the Westbury Formation bone beds than ichthyosaur bones (Storrs, 1994, 1999). The Rhaetian bone beds sample only two sauropterygian clades, the plesiosaurs and placodonts (Nordén et al., 2015), but not their typical Middle and Late Triassic relatives, the pachypleurosaurs and nothosaurs. Plesiosauria diversified rapidly in the earliest Jurassic (Benson et al., 2012), and the Rhaetian specimens presumably represent some of the earliest, as yet poorly documented, members of the clade. As with the ichthyosaur elements, plesiosaur bones in the bone beds are disarticulated and often abraded following transport, and they cannot be assigned to genera or species (Storrs, 1994, 1999).

4.7.2.1. Teeth

In the collection there are 16 plesiosaur teeth, all incomplete, ranging in size from 5–20 mm. One example of a mid-sized tooth (Fig. 14a and b) is a curved, elongated cone,

circular in cross section, with numerous, precisely spaced and thin apicobasal striations. The smallest teeth can be relatively stouter and more recurved (Benson et al., 2012).

4.7.2.2. *Vertebrae*

The Curtis HFQ collection includes four plesiosaur vertebrae, ranging in dimensions from 40–70 mm. The vertebrae are cylindrical with flat ends and paired ventral foramina, and the neural arches are usually fused to the centra.

One specimen (Fig. 14c–f) is an entire centrum with an incomplete fused neural arch, lacking the neural spine and postzygapophyses. The parapophyses are small, pointed processes on the ventral portion of the centrum. The diapophyses are less clear. This vertebra is interpreted as a cervical centrum, because the articular facets for the rib are entirely on the centrum.

Another specimen (Fig. 14g and h) is less complete, comprising just the centrum. The articular face shows the oval shape, expanded laterally, and the facets for attachment of the neural arch are clear in dorsal view (Fig. 14h). The oval shape of the centrum suggests that this was probably a dorsal vertebra.

4.7.3. *Pachystropheus rhaeticus* E. von Huene, 1935

Pachystropheus is an enigmatic reptile, classified variously as a choristodere or a thalattosaur (Storrs and Gower, 1993; Storrs et al., 1996; Renesto, 2005; Allard et al., 2015), and common in certain Rhaetian bone beds, but especially those where there has been modest physical transport and abrasion (Storrs, 1994, 1999; Trueman and Benton 1997; Allard et al., 2015).

One limb bone (Fig. 15a–d) appears to be a right femur, by comparison with femora figured by Storrs et al. (1996, figs. 12, 13). The slender proportions and the 90° twist halfway

along the diaphysis (Fig. 15b) are diagnostic. The proximal head is missing, but the gently curved inner trochanteric crest is evident. The distal end is more complete, but appears to lack the articular faces. The specimen is relatively large, being 80 mm long, compared to 63 mm for the holotype femur (Storrs et al., 1996, p. 339). There are no teeth referable to *Pachystropheus* found in HFQ, or to our knowledge anywhere in the British Rhaetian deposits. However, if *Pachystropheus* is an edentulous thallatosaur similar to *Endennasaurus*, as suggested by Renesto (2005), then this would account for the absence of teeth.

4.7.4. Unknown tetrapod fossils

4.7.4.1. Unknown reptile bones

In the collection, there are many unknown bone fragments with a size range from less than 10 mm to several decimetres.

One specimen is an L-shaped fragment (Fig. 15e and f), greatly abraded, and in which there is no particular feature that would aid identification. In the probable medial view a medial ridge is visible (Fig. 15f). It could be an abraded skull bone, such as a postorbital, with the curved edge bordering a fenestra.

Another specimen (Fig. 15g and h) resembles a rib whose posterior part is incomplete, while the proximal head recalls the capitulum and tuberculum, although quite eroded. However, it is impossible to determine the animal to which this belonged.

4.7.4.2. Archosaur tooth - ?Thecodontosaurus

A possible archosaur tooth is represented by a single broken, arrowhead-shaped specimen (Fig. 15i and j), which is flattened and has sharp-edged anterior and posterior margins. There are approximately 11 serrations from the broken base of the tooth to the apex along one of these sharp edges, spaced about 8 serrations per mm. The tooth margins are

substantially abraded, so the overall shape of the serrations cannot be discerned, and there are apparently no serrations on the other margin, but they might have been removed by abrasion. The centre of the tooth has a small half-cone-shaped protrusion. The other face of the tooth has been severely worn to reveal the internal structure of the tooth. No root is attached. The specimen is 1.7 mm high and 0.8 mm wide.

This tooth is probably reptilian, and possibly from an archosaur. The leaf-shaped morphology of the tooth and the broad serrations indicate that its possessor was a herbivore, and it may be a much abraded *Thecodontosaurus* tooth, by comparison with the fragmentary, but less abraded, specimens illustrated by Foffa et al. (2014, fig. 3I–L). The size is the same, as is the indication of overall tooth shape as a symmetrical, leaf-shaped tooth in lateral view.

4.8. Vertebrate coprolites

The collection from HFQ includes several hundred coprolites. Many specimens are broken and sizes vary from 3 mm to over 31 mm long. A detailed analysis of the range of coprolite morphologies represented in the ichnofauna is beyond the scope of this paper, but several types are represented in the collection; indeed, it is clear that the initial classification scheme for Rhaetian coprolites proposed by Duffin (1979) and repeated in Swift and Duffin (1999) may have to be extended. Many of the coprolites are round to sub-oval, whilst others are spindle-shaped, elongate cylinders or flattened (Fig. 16). Some specimens show clear evidence of internal spiral morphology with the final whorl lapped around the edge of the specimen (Fig. 16a). In a small number of cases, there are superficial markings conferred on the faecal material by the intestinal walls as it passed down the digestive tract, including spiral lineations on the outer surface of the specimens (Fig. 16b).

Vertebrate inclusions are common, mostly consisting of isolated osteichthyan scales, some of which stand out from the coprolite surface (Fig. 16c) whilst others are completely

enclosed by faecal matrix within which they have a preferred orientation (Fig. 16d). One noteworthy specimen (Fig. 16e) contains at least two vertebrae of *Pachystropheus rhaeticus* plus some ornamented bone, the first coprolite recorded from the British Rhaetian containing remains of this particular reptile.

4.9. Invertebrates

All Westbury Formation bone beds include rare invertebrate fossils mixed with the teeth and bones (Storrs, 1994; Swift and Martill, 1999). These include 25 or more species of bivalves, several species of crustaceans, rare brachiopods, ophiuroids, echinoid spines, and rare ammonites, conodonts, and foraminifera. In the HFQ collection, unusually, the most abundant fossils are gastropods, with rarer echinoids. Many specimens could be identified to genus and species, but the majority could not be identified more closely than to order. These specimens are all from the Curtis collection from bed 9, and many were presumably hand picked before the sediment was acid treated, although phosphatised gastropods and crinoid ossicles survive the treatment. This means that the counts of invertebrates are unlikely to be representative of what was originally preserved.

4.9.1. Gastropods

Gastropod specimens are all small, less than 20 mm across, and they were identified under the light microscope. There are 104 specimens of which 81 could be identified, and 23 were unassigned.

4.9.1.1. *Cylindrobullina* von Ammon, 1878

The most abundant gastropod is *Cylindrobullina*, which accounts for approximately 50% of the specimens (Fig. 17a–d). This genus, represented by specimens 3–9 mm in height,

is readily distinguished by the large oval last whorl, which comprises 80% of the shell volume. Whorls are convex and separated by grooved sutures that are almost horizontal. In approximately 10% of these specimens, there is a pinch at the base of the last whorl on the outer lip, and this is identified as the siphonal canal. Here siphons may have been protruded. *Cylindrobullina* is found both as more or less complete, phosphatised specimens (Fig. 17a and b) or as steinkerns, the internal mould of the shell after the shell material has been removed (Fig. 17c and d).

There are four Rhaetian species of *Cylindrobullina* (Barker and Munt, 1999), all of them originally found and most abundant from sites around Bristol and Beer Crocombe and Watchet, Somerset. The species are distinguished by their overall shape, ranging from globular to cylindrical, the proportion of the last whorl, ranging from 0.67–0.8 of the length of the shell, the shape of the aperture, whether oval or slit-like, and overall size. The four species might include varieties or growth stages of each other (Barker and Munt, 1999, p. 81). *Cylindrobullina* is known extensively also from the Early Jurassic (Gründel et al., 2011).

4.9.1.2. Rarer gastropods

The remainder of the gastropods are rare, with often only one to six specimens of each genus. Six specimens are identified as *Discohelix suessii* (Moore, 1861), on the basis of its discoidal geometry in one plane and wide aperture (Fig. 17e). Two specimens are assigned to *Promathildia rhaetica* (Moore, 1861) on the basis of the tall turreted geometry of the spire, with ornamentation occurring as three dark spiralling threads parallel to the suture lines (Fig. 17f). One specimen is assigned to *Pleurotomaria* based on the possible presence of a calcified selenizone. Along the suture lines there was preferential mineralization forming a prominent band spiralling down the shell, perhaps representing the previous position of the slit band where siphons could have protruded.

A further unexpected find is a tiny globular specimen, abraded round the edges, but showing steep spiral portions (Fig. 17g), similar to *Glabrocingulum*, a genus typical of the late Palaeozoic, and so possibly reworked from the underlying Carboniferous Limestone, but the genus has been identified also in the Triassic, including the Late Triassic Antimonio Formation of New Mexico, USA (Stanley et al., 1994).

4.9.2. Echinoid spines and plates

Echinoderms have been reported only occasionally from Rhaetian bone beds, but Swift (1999) notes that they are relatively common in sieved residues, and this is also the case for the Curtis collection from HFQ. Here, echinoids are represented by 176 specimens, of which 172 are spines. The spines (Fig. 17h) are prolate and broken portions are no more than 5 mm in length, with a diameter of approximately 1 mm. The spines are often fragmented, but in some better-preserved specimens the base of the spine shows the acetabulum. The base shows the spine was solid. The neck is smooth, and slopes out to a broad ridge at the base of the shaft, which is covered with short spines arranged in longitudinal ridges. The morphology of the spines suggests they come from cidaroid echinoids.

Three specimens are identified as echinoid plates, potentially a pore plate and two interambulacral plates. These two plates (Fig. 17i and j) are 2.8 mm wide, square-shaped and convex, showing seven rounded convex bosses on the external surface, and smoothly concave internal face that shows the perforated pattern of the stereom.

4.9.3. Ophiuroid arm vertebral ossicles and plates

There are approximately 215 ophiuroid specimens, a mixture of 128 arm vertebral ossicles and plates. The arm vertebral ossicles (Fig. 17k–n) can be assigned tentatively to genera and species because of diagnostic characters of shape and articulating structures. One

broad ossicle (Fig. 17k) is superficially similar to *Antiquaster*, a Devonian brittlestar (Kesling, 1971, fig. 1), based on being about three times as wide as tall, and bearing two broad, low-relief articulating surfaces on either side of a midline depression. The other arm vertebral ossicle morphs are similar, being more equidimensional, and with broad, flat articular faces (Fig. 17l–n). The tallest morph (Fig. 17m and n) is similar to a proximal vertebral ossicle of *Aplocoma agassizi*

Ophiuroid plates include a broad array of forms (Fig. 17o–t). The simple curved plate (Fig. 17o) is similar to a proximal lateral arm plate of *Aplocoma agassizi* (von Münster, 1839) from the Rhaetian of the Netherlands (Thuy et al., 2012, fig. 3H, I).

5. Faunal composition

The specimens in the Curtis collection from HFQ were not all clearly allocated to horizons, and so we report approximate proportions of materials from the whole collection, and from those clearly labelled as being from Curtis' bed 9. The total collection in both BRSMG and BRSUG (Fig. 18a) consists of 26,237 fossils, of which 17,443 are osteichthyan remains, forming 66% of the collection, 3,147 chondrichthyan remains (12%), 422 marine reptile remains (2%) and 5,225 indeterminate remains, comprising fragments or unclassifiable specimens (20%). The bed 9 collection (Fig. 18b) lacks the larger elements, and comprises 40% *Gyrolepis albertii* teeth, 25% *Severnichthys acuminatus* teeth, 25% osteichthyan scales, and 10% chondrichthyan teeth and scales.

In our collections from the 2014–2015 excavated section (Fig. 4a), there is considerable variation in specimen count from bed to bed (Fig. 19), with most abundant fossils in our HFQ-19 bed (the basal bone bed) and in our HFQ-12 bed (Curtis bed 9), and lower counts in the other beds from similar sediment samples that were similarly processed. Comparing the samples (Tables 1, 2), there are some common taxa, with for example 4–16% *Gyrolepis*

albertii teeth and 2–29% *Severnichthys acuminatus* teeth, 0–34% scales, and 4–15% denticles in all beds. The variations in proportions of these taxa do not show any particular temporal pattern, with highest counts of *Gyrolepis albertii* in HFQ-16, *Severnichthys acuminatus* in HFQ-2, scales in HFQ-11, and denticles in HFQ-1 and HFQ-14, so the variations are likely mainly taphonomic and reflective of sample size. More interesting are the taxa that appear only in certain horizons. For example, *Rhomphaiodon minor* and rare *Vallisia coppi* occur in the basal bone bed only. There is a repeat of very rare *Lissodus minimus*, *Rhomphaiodon minor*, and *Sargodon tomicus* in HFQ-2, and the former in HFQ-14. *Duffinselache* is reported only from HFQ-16 and the immediately succeeding HFQ-1, but from only one specimen in each, while durophagous teeth were found only in HFQ-11. *Pseudocetorhinus pickfordi* occurs throughout the succession, both as jaw teeth and as gill raker teeth. Note that, slightly differently to our findings, Curtis recovered *Lissodus*, *Vallisia*, and *Sargodon* from his bed 9 (our HFQ-12).

6. Discussion

6.1. Assessing the assemblage composition

The description of faunal composition relies on identification of taxa and counting. Most of the teeth are sufficiently distinctive to be identified with reasonable confidence, but one common problem was in distinguishing teeth of *Gyrolepis albertii* from those of *Severnichthys acuminatus*. The main distinction is that *S. acuminatus* teeth have ornamentation, whereas *G. albertii* teeth are unornamented (Fig. 7a–c). There is a problem in identification if the teeth are abraded. Further, we could use only standard assumptions in previously published works in making our identifications.

In the case of *Severnichthys*, heterodonty has been recognized and the different morphs brought together under a single name (Storrs, 1994). However, heterodonty and sexual

dimorphism are widespread in **fishes** today, and some of the other individually named taxa might **also** turn out to be variants of teeth of a single taxon.

A further difficulty was in counting specimens and what constitutes a single specimen, tooth or scale. Typically, for chondrichthyan teeth, a whole tooth was classed as a tooth with the central cusp present with some portion of root. Some morphotypes, however, rarely had any root preserved, such as *Lissodus minimus*, and so for this taxon only the crown with a portion of the central cusp was required for counting. Osteichthyan teeth were more varied in morphology, and so the qualification for a whole tooth varied as well. We followed counting rules (see Section 3.4) used in previous studies (Van den Berg et al., 2012). In the end, the counts for scales and vertebrae represent simply the total numbers and take no account of the numbers of these elements per individual fish. Thus, the totals of teeth, vertebrae, and scales are massive overestimates of the numbers of individuals that would have been required to provide such numbers of elements, but the relative numbers are probably reasonably indicative of which taxa were most common, and which most rare.

Apart from the counting problems, there are many other biological and geological biases **in such bone bed assemblages** (Heckert, 2004; Rogers & Kidwell, 2007). Chondrichthyans, for example, shed their teeth freely throughout life, and **more frequently than** a typical osteichthyan. The robustness of elements also affects their survival through transport and burial. Here, we focus on teeth, which survive transport and fossilisation well, as well as bony denticles and thick, bony scales. Teeth and scales possess hypermineralised hard tissues such as enamel, acrodin and dentine and are intrinsically more robust and therefore have a higher preservation potential than the rather more cellular, lacunate tissues of bony elements. Other elements, such as the vertebrae, ribs, and skull bones of osteichthyans have not been identified – either they were winnowed and transported elsewhere, or they were abraded and broken, **or even destroyed by digestive acids**. The intensive sampling by

Mike Curtis and by our team can exclude a third option, that these unidentified elements were found but not identified – we noted all bone fragments, and very few look like abraded osteichthyan vertebrae, ribs, or skull bones.

6.2. The HFQ ecosystem

The data suggest that the HFQ palaeocommunity was dominated by *Gyrolepis albertii* and *Severnichthys acuminatus* throughout. The maximum counts of these taxa, however, do not exceed 30–36%, so the numbers could indicate a balanced ecosystem in which no single species dominates exclusively. Both *Gyrolepis* and *Severnichthys* were predators, adapted to snatching other fishes with their numerous long, pointed teeth. *Severnichthys* was the larger of the two, estimated at 1 m long (Storrs, 1994), and therefore capable to preying on all the other fishes, and even small reptiles. Because of its size and likely weight, *Severnichthys* may have been an ambush predator, lurking among rocks or seaweed, and lunging at prey that passed by.

Some Rhaetian bone bed sites have yielded large numbers of osteichthyans with durophagous dentitions (e.g. Korneisel et al., 2015). Here, however, we report only very small numbers of *Sargodon* with its broad, polished teeth (Fig. 7e–h), and a few examples of durophagous tooth plates (Fig. 7j), bearing numerous rounded, circular teeth embedded in a broad jaw bone element. There were abundant benthic invertebrates at HFQ for the durophagous fishes to eat, including gastropods and echinoderms, as well as bivalves and brachiopods, and arthropods, which have not been reported from HFQ, but which are known from other Rhaetian bone beds (Swift and Martill, 1999). The bivalve *Gervillella praecursor* was noted in HFQ-2 during excavation, but was lost to acid treatment of the samples; this is the key horizon for *Sargodon tomicus*, a possible shell-crushing predator. Durophagous diets first arose in the Late Triassic, enabled by the origin of a new clade of osteichthyans, the

Neopterygii, with their derived jaw systems in which the maxilla was free posteriorly and could become equipped with powerful muscles to bring pressure on toothplates that were used to rasp and crush shells (Lombardo and Tintori, 2005).

The HFQ sharks, *Rhomphaiodon*, *Duffinselache*, *Lissodus*, *Pseudocetorhinus*, and *Synechodus* have been reported widely in the British Rhaetian (Storrs, 1994; Duffin, 1999; Allard et al., 2015; Korneisel et al., 2015). The teeth are generally small, suggesting that these sharks were also small, although their original body sizes and shapes are unknown as no complete specimens have been identified. These shark taxa show a broad range of tooth shapes, from the low, broad teeth of *Lissodus* to the triangular, pointed teeth of *Pseudocetorhinus*, and these shapes presumably indicate adaptation to different diets. *Lissodus* was interpreted (Cuny and Benton, 1999, p. 200) to have teeth of ‘crushing type, indicating more opportunistic feeding behaviour’, while *Pseudocetorhinus* may have been a filter feeder (Duffin, 1999). The other sharks may have been adapted for clutching and piercing prey animals, both fishes and invertebrates.

The marine reptiles from HFQ, the ichthyosaurs, and plesiosaurs, were predators, as indicated by their pointed teeth. Although the teeth and vertebrae are isolated, their relatively small size indicates body lengths of 1–2 m, in line with other findings from the Rhaetian. There were rare, enormous individuals with vertebrae 20 cm across (Storrs, 1994). The diet of *Pachystropheus* is less certain because there are very few skull remains. In life, *Pachystropheus* was 1–2.5 m long, and whether it is identified as a choristodere or a thalattosaurian, it was probably also a carnivore, presumably feeding on fishes. If it lacked teeth, it might have fed on fish fry, small crustaceans, or anything soft-bodied (Renesto, 2005).

Invertebrates are rare in the HFQ collection, but they include typical forms of gastropods and echinoderms. Missing are the corals and arthropods (ostracods, barnacles,

lobsters) found at other localities (Swift and Martill, 1999), which could suggest that the HFQ bone beds contain only a limited representation of what was originally present on the sea floor thanks to transport, abrasion, and winnowing, but is **as** likely a result of the destruction of calcareous-shelled organisms by our acid treatment of the sediment for microvertebrates,

6.3. *Variation through time in Rhaetian bone bed assemblages – taphonomy or evolution?*

In many older papers, only the basal Rhaetian bone bed was described, and little was said about the occurrence of bones higher in the section. Sykes (1977) summarised 40 Rhaetian sections recorded in earlier works, distributed from Devon to Yorkshire, and he showed the frequent occurrence of higher bone beds, but he identified these as ‘secondary’ or ‘scatter’ bone beds. The largest number of separate bone beds was reported from the Westbury Formation at Barrow upon Soar in Leicestershire, which showed eight bone beds in all, the basal ‘primary’ bone bed, three higher ‘secondary’ bone beds, and four ‘scatter’ and ‘trace’ bone beds. Sykes (1977, p. 200) noted that ‘All Rhaetic bone-beds have some features which suggest that they have been derived from a previously deposited source, although some primary depositional features may also be retained’. He noted that the primary bone beds, namely examples of the basal Westbury bone bed, contain coprolites, evidence for minimal transport, whereas higher, ‘secondary’ bone beds show more signs of transport and abrasion. However, this scheme does not really work because the basal bone bed in many locations comprises a mix of locally derived (Blue Anchor Formation mud clasts, coprolites) and multiply transported (abraded bones) debris, while other basal bone beds show remarkably different amounts of breakage and abrasion of bones, ranging from massively abraded, rounded bone pebbles at Aust to delicate, undamaged slender bones at Westbury Garden Cliff (Trueman and Benton, 1997). **Mixing of elements transported different distances, and even the association of freshwater lungfish remains with marine fishes and ichthyosaurs in a single**

bone bed, are most likely all coeval, not mixed from deposits of various ages. Further, the higher bone beds in the Westbury Formation, such as bed 9 at HFQ, often show less evidence of abrasion, and finer, more delicate fossils, than in the basal bone bed.

Subsequent reviews of the Rhaetic vertebrates (e.g. Storrs, 1994; Martill and Swift, 1999) did not follow Sykes' (1977) classification, but Macquaker (1994) and Martill (1999) argued that the Rhaetic bone beds comprise bone debris sourced from 'slightly older deposits'. They interpreted the series of Rhaetic bone beds as genetically linked by a transgressive lag depositional model: 'In this model, a transgressing sea derives clasts, including skeletal phosphates, from pre-existing sediments and incorporates them into first a basal bone bed and, further offshore from the site of erosion, into thinner intraformational bone beds' (Martill, 1999, p. 61). Neither paper provides evidence of reworking of a pre-existing fossiliferous bed, for example the occurrence of blocks of matrix containing bones, and it is not clear why the materials could not all be freshly transported, some of the materials over a considerable distance, or through several cycles, rather than from 'pre-existing sediments'. The hint in the quotation from Martill (1999) that all the bone beds throughout the Westbury Formation could be part of a single, long-term transgressive action that deposited first the basal bone bed, and then, later, the higher bone beds, is also unwarranted. There is no evidence that the Westbury Formation bone-bearing horizons located stratigraphically higher than the basal bone bed are sedimentologically linked. The temporal duration of the Westbury Formation was estimated by Macquaker (1994) as 1.66–5 Myr, although we will consider a maximum of 2 Myr (assuming the Westbury Formation is half the Rhaetic, matched in duration by the overlying Lillstock Formation; total duration of Rhaetic, 4.4 Mr: Maron et al., 2015), and so many cycles of sedimentation are likely included, and much time is unrepresented by sediment.

Of the numerous Rhaetian bone beds, only the basal bone bed is likely to represent a single, roughly correlatable event, even though it was likely time-transgressive over years or decades, but presumably not thousands or millions of years. The basal Rhaetian bone bed traverses much of central and western Europe, and shows substantial local variations in thickness, mean clast size, and the nature of locally derived debris (Macquaker, 1994; Suan et al., 2012). In some places it is absent, as shown by Curtis (1981), often because the waters and traction loads swept around minor local topographic highs, such as upstanding ridges of harder Carboniferous sediment in the Chipping Sodbury quarries. The traction loads of heavy phosphatic debris could travel substantial distances and so larger bone fragments became massively abraded, whereas in other locations, fish and reptile debris was carried only a short distance, before being dumped and then winnowed. In places, small bones and teeth became trapped in cracks in the underlying lithified Carboniferous limestone, or were reworked actively by contemporary, Rhaetian-age callianassid shrimps into *Thalassinoides* burrow systems that penetrated unlithified Upper Triassic sediments (Korneisel et al., 2015).

Bone beds occurring higher in the sections presumably each have their own story, but there is again no evidence that they were reworked from lower horizons, including the basal bone bed, as has been suggested (Sykes, 1977; Martill, 1999). These higher bone beds are just as likely to show minimal evidence of transport as to yield abraded bones. There is no evidence that the Westbury Formation did not accumulate as generally fine-grade sediment and without intervening erosive episodes that reworked older sediment. Whether any of the higher-occurring bone beds, such as bed 9 at HFQ, can be correlated over wider areas has yet to be demonstrated. Key evidence that the various Westbury Formation bone beds are not reworked variants of the basal bone bed is the substantial changes in faunal content (Fig. 20; Tables 1, 2) and the fact that there is no evidence for increasing abrasion, nor of any directional trend in specimen size from coarser to finer up-section. At HFQ, and elsewhere,

mean clast size diminishes from the basal bone bed to higher bone beds, but abrasion is actually less marked in bed 9 than the basal bone bed at HFQ.

Here, we reported bone occurrences from 17 levels in the Westbury Formation (Fig. 19), but five of these yielded negligible finds, so we count 12 bone-bearing levels, clustered in the lowest and highest metres of the section. Some occurrences, however, are sparse, and probably only the basal bone bed and our HFQ-12 would count as rich enough to be identified as bone beds, with the others sampling some vertebrate remains, but not in the form of concentrated lag deposits, the general interpretation of the Rhaetian bone beds (Martill, 1999).

The various Westbury Formation bone beds differ in their taxon lists and relative proportions of the different species, reflecting a mix of taphonomic factors, such as sampling from different contemporary facies and differential sorting, as well as perhaps some biological factors (evolution through the 2 Myr of deposition, or palaeoecology). Some authors (e.g. Savage and Large, 1966) had suggested there was little change in the faunas through the time span represented by the Westbury Formation or the Westbury Formation plus the overlying Cotham Member, and others (e.g. Storrs, 1994; Swift and Martill, 1999) did not speculate on whether faunas changed or not through the Rhaetian. However, our work on HFQ, and other studies (e.g. Sykes, 1977; Duffin, 1980; Allard et al., 2015) confirm that there were some changes both in the taxon lists and in relative proportions of the more common elements.

In our work, and in unpublished reports by Mike Curtis, we confirm that there was a change in dominance of the microvertebrate assemblages from 40% chondrichthyans, especially *Rhomphaiodon minor* and *Lissodus minimus*, in the basal bone bed to 15–20% in HFQ-16, HFQ-2, and HFQ-12 (bed 9): the difference was made up by increases in abundance of the osteichthyans *Gyrolepis albertii* and *Severnichthys acuminata* (Fig. 20). We argue that

these changes in proportions have **some** biological significance, and are not **purely** taphonomic artefacts, for **three reasons**: (1) **the** same patterns are reported from several Rhaetian successions around Bristol (e.g. Allard et al., 2015; Lakin et al., 2016); (2) the overall sedimentary regime throughout the Westbury Formation is comparable, so all the sources of error in matching numbers of micro-teeth to numbers of fishes (see Section 6.2 below) would probably apply equally throughout; and (3) the teeth, scales, and denticles of the cartilaginous and bony fishes all fall within the same range of sizes and shapes, so that it would be hard to construct a physical, taphonomic model to effect the switch in group dominance.

Duffin (1980) was first to discriminate the faunas within different British Rhaetian bone beds. At Chilcompton, he noted the dominance of the chondrichthyans *Rhomphaiodon minor* and *Lissodus minimus* in the basal bone bed, comprising almost 60% of the collection, and these taxa were ‘virtually absent’ from the bone bed he reported at the base of the Cotham Member, the younger fauna being **dominated by** *Gyrolepis albertii* (78% of all teeth identified) and *Severnichthys acuminatus* (21%). Similar results were noted by Allard et al. (2015) in their study of the Manor Farm Quarry section. There, as elsewhere, the basal bone bed yielded much more abundant fossils per kg of sampled rock than the younger bone beds, and certain taxa (*Rhomphaiodon minor* and *Pseudodolatias barnstonensis*) are found only in the basal Westbury Formation bone bed, or occur in the basal bone bed and the bone bed at the top of the Westbury Formation, equivalent to HFQ bed 9 of Curtis (*Lissodus minimus*). At Manor Farm, *Vallisia coppi* does not occur in the basal bone bed, but only in samples from the middle of the Cotham Member. However, unlike HFQ, *Duffinselache holwellensis* does not occur low in the Westbury Formation at Manor Farm Quarry, but only in the bone bed at the top of the Westbury Formation, and in the Cotham Member, in smaller quantities (Allard et al., 2015, table 1).

Despite these common findings among the most abundant taxa represented by microremains, the basal Westbury Formation bone bed can show considerable variation from site to site, even between geographically close localities. For example, the classic basal bone bed at Aust Cliff has yielded taxa that have not been found at HFQ despite intensive sampling by Mike Curtis over many years, and with the benefit of extensive mechanical ground clearing operations. Taxa such as *Pseudodolatias barnstonensis*, *Nemacanthus monilifer*, *Ceratodus latissimus*, and *?Psephoderma alpinum* from Aust Cliff have not been found at HFQ.

Unique elements of the higher bone bed in the Westbury Formation, Curtis' bed 9, include the neoselachian sharks *Pseudocetorhinus pickfordi* and *Synechodus rhaeticus*, and tooth plates of durophagous osteichthyans. Further, and unexpectedly, we report substantial changes in the relative proportions of the two morphs of *Severnichthys acuminatus* between the basal and higher bone beds. The '*Birgeria*' morph is found in both beds, being most abundant in the lower bone bed, and the '*Saurichthys*' morph is common in the basal bone bed, but very rare in the upper. This pattern of changing relative abundances of the two morphs was reported also from Manor Farm by Allard et al. (2015, p. 773), and so **might** suggest reconsideration of whether these two tooth forms really do belong to a single taxon, as proposed by Storrs (1994). **The two tooth types are of different sizes, and so their presences and absences might be partly taphonomic, but** *Birgeria* and *Saurichthys* occur as complete skeletons from the Late Triassic of Bergamo, North Italy (D.I.W., pers. obs.), and a comparison between the HFQ *Severnichthys* morphs and the Italian specimens from a very similar ecosystem would be instructive.

Changing faunas through the Rhaetian bone beds were also noted by Cuny et al. (2000) from a Rhaetian succession at Lons-le-Saunier in Jura, France. They sampled microvertebrates from three horizons, and found that the lowest bed (R11) had a shark fauna

dominated by *Lissodus minimus* and only 8% neoselachians, mainly *Rhomphaiodon minor*. In a higher bone bed (R22) neoselachians comprised 25% of the assemblage of microteeth, represented mainly by the durophagous *Synechodus rhaeticus*. ‘*Birgeria*’-type teeth occurred throughout, but reduced in dominance upwards through the three horizons. Among durophages, *Sargodon tomicus* increased in abundance from bed R11 (7% of total bony fish teeth) to bed R22 (30%).

The increase in numbers of neoselachians may be a local phenomenon, but it is in line with the worldwide diversification of that clade through the Triassic and Jurassic (Cuny and Benton, 1999). The increase in durophagous forms upwards through the Westbury Formation may be another real evolutionary trend, showing expansion of niches occupied by both neoselachian sharks and osteichthyans as they broadened their diet to include hard-shelled taxa as well as softer-bodied organisms. Part of the evidence for the Mesozoic Marine Revolution (Vermeij, 1977) was an increase in predatory specialisations to deal with otherwise well protected prey.

The fact that similar faunal changes have been detected in the Rhaetian successions of several localities in England and in France suggests there may be a commonality that is partly biological. Local palaeoecology or taphonomy could account for such changes in proportions and taxa, but probably not over a wide area of Europe. Further closely documented examples will help test this further.

Acknowledgements

EMM thanks Crispin Little (University of Leeds) for help and advice during her BSc dissertation work. We also thank Ian Strachan and James Veakins from Hanson Aggregates, who provided access to the site in summer 2014 and 2015. We thank Isla Gladstone and Deborah Hutchinson at BRSMG for assistance with their collections, and of course Mike and

Sharon Curtis for their heroic efforts in amassing such a huge collection of microvertebrates from HFQ and presenting them in such good order. We thank David Martill and Andy Heckert for their very helpful reviews.

References

- Agassiz, L.J.R., 1833–1844. *Recherches sur les Poissons Fossiles. Tome 3 Concernant l'Histoire de l'Ordre des Placoïdes*. Imprimerie Petitpierre, Paris 390 + 34 pp.
- Allard, H., Carpenter, S.C., Duffin, C.J., Benton, M.J., 2015. Microvertebrates from the classic Rhaetian bone beds of Manor Farm Quarry, near Aust (Bristol, UK). *Proceedings of the Geologists' Association* 126, 762–776 (doi: 10.1016/j.pgeola.2015.09.002).
- Andreev, P.S., Cuny, G., 2012. New Triassic stem selachimorphs (Chondrichthyes, Elasmobranchii) and their bearing on the evolution of dental enameloid in Neoselachii. *Journal of Vertebrate Paleontology* 32, 255–266.
- Barker, M.J., Munt, M.C. 1999. Gastropods. In: Swift, A., Martill, D.M. (Eds.), *Fossils of the Rhaetian Penarth Group*, vol. 9. Palaeontological Association Field Guide to Fossils, pp. 75–82.
- Benson, R.B.J., Evans, M., Druckenmiller, P.S., 2012. High diversity, low disparity and small body size in plesiosaurs from the Triassic– Jurassic boundary. *PLoS ONE* 7, e31838.
- Benton, M.J., Forth, J., Langer, M.C., 2014. Models for the rise of the dinosaurs. *Current Biology* 24, R87–R95.
- Benton, M.J., Schouten, R., Drewitt, E.J.A., Viegas, P., 2012. The Bristol Dinosaur Project. *Proceedings of the Geologists' Association* 123, 210–225.
- Boomer, I., 1991a. On *Ektyphocythere cookiana* (Anderson). *Stereo-Atlas of Ostracod Shells* 18, 113–116.

- Boomer, I., 1991b. On *Ogmoconchella martini* (Anderson). Stereo-Atlas of Ostracod Shells 18, 121–124.
- Brusatte, S.L., Nesbitt, S.J., Irmis, R.B., Butler, R.J., Benton, M.J., Norell, M.A., 2010. The origin and radiation of dinosaurs. *Earth-Science Reviews* 101, 68–100.
- Cappetta, H., 1987. Volume 3B: Chondrichthyes II. In H.-P. Schultze (Ed.), *Handbook of Palaeoichthyology*. Gustav Fischer Verlag, Stuttgart.
- Cappetta, H., 2012. Volume 3E: Chondrichthyes. Mesozoic and Cenozoic Elasmobranchii: Teeth. In: Schultze, H.-P. (Ed.), *Handbook of Paleoichthyology*. Verlag Dr Friedrich Pfeil, München.
- Chen, Z.Q., Benton, M.J., 2012. The timing and pattern of biotic recovery following the end-Permian mass extinction. *Nature Geoscience* 5, 375–383.
- Cuny, G., Benton, M.J., 1999. Early radiation of the neoselachian sharks in western Europe. *Geobios* 32, 193–204.
- Cuny, G., Hunt, A.P., Mazin, J.-M., Rauscher, R., 2000. Teeth of enigmatic neoselachian sharks and an ornithischian dinosaur from the uppermost Triassic of Lons-le-Saunier (Jura France). *Paläontologische Zeitschrift* 74, 171–185.
- Cuny, G., Risnes, S. 2005. The enameloid microstructure of the teeth of synechodontiform sharks (Chondrichthyes: Neoselachii). *Palarch's Journal of Vertebrate Palaeontology* 3, 8–19.
- Curtis, M.T., 1981. The Rhaetian–Carboniferous limestone unconformity at Chipping Sodbury Quarry, Chipping Sodbury, Avon. *Proceedings of the Bristol Naturalists' Society* 40, 30–34.
- Deenen, M.H.L., Ruhl, M., Bonis, N.R., Krijgsman, W., Kürschner, W.M., Reitsma, M., Van Bergen, M.J., 2010. A new chronology for the end-Triassic mass extinction. *Earth and Planetary Science Letters* 291, 113–125.

- Delsate, D., Duffin, C.J., Weis, R., 2002. A new microvertebrate fauna from the Middle Hettangian (Early Jurassic) of Fontenoille (Province of Luxembourg, south Belgium). *Memoirs of the Geological Survey of Belgium* 48, 1–83.
- Donovan, D., Curtis, M., Curtis, S., 1989. A psiloceratid ammonite from the supposed Triassic Penarth Group of Avon, England. *Palaeontology* 32, 231–235.
- Duffin, C. 1979. Coprolites: a brief review with reference to specimens from the Rhaetic Bone Beds of England and South Wales. *Mercian Geologist* 7, 191–204.
- Duffin, C.J., 1980. The Upper Triassic section at Chilcompton, Somerset, with notes on the Rhaetian of Somerset in general. *Mercian Geologist* 7, 251–268.
- Duffin, C.J., 1982. Teeth of a new selachian from the Upper Triassic of England. *Neues Jahrbuch für Geologie und Paläontologie, Monatshefte* 1982, 156–166.
- Duffin, C.J., 1985. Revision of the hybodont selachian genus *Lissodus* Brough (1935). *Palaeontographica Abteilung A* 188, 105–152.
- Duffin, C.J., 1993. Teeth of *Hybodus* (Selachii) from the Early Jurassic of Lyme Regis, Dorset (southern England): preliminary note. *Belgian Geological Survey. Professional Paper* 264, 45–52.
- Duffin, C.J. 1998a. New shark remains from the British Rhaetian (latest Triassic). 1. The earliest Basking shark. *Neues Jahrbuch für Geologie und Paläontologie, Monatshefte* 1998, 157–181.
- Duffin, C.J., 1998b. New shark remains from the British Rhaetian (latest Triassic). 2. Hybodonts and palaeospinacids. *Neues Jahrbuch für Geologie und Paläontologie, Monatshefte* 1998, 240–256.
- Duffin, C.J., 1999. Fish. In: Swift, A., Martill, D.M. (Eds.), *Fossils of the Rhaetian Penarth Group*, vol. 9. *Palaeontological Association Field Guide to Fossils*, pp. 191–222.

Duffin, C.J., 2001. Synopsis of the selachian genus *Lissodus* Brough, 1935. Neues Jahrbuch für Geologie und Paläontologie, Abhandlungen 221, 145-218.

Duffin, C.J., 2010. Chondrichthyes. In: Lord, A.R. & Davis, P.G. (Eds.) Fossils from the Lower Lias of the Dorset Coast. Palaeontological Association Field Guide to Fossils, pp. 317–340.

Duffin, C.J., Coupatez, P., Lepage, J.C., Wouters, G., 1983. Rhaetian (Upper Triassic) marine faunas from le golfe du Luxembourg in Belgium (preliminary note). Bulletin de la Société Belge de Géologie 92, 311–315.

Duffin, C.J., Ward, D.J., 1993. The Early Jurassic palaeospinacid sharks of Lyme Regis, southern England. Belgian Geological Survey Professional Paper 264, 53–102.

Foffa, D., Whiteside, D.I., Viegas, P.A., Benton, M.J., 2014. Vertebrates from the Late Triassic *Thecodontosaurus*-bearing rocks of Durdham Down, Clifton (Bristol, UK). Proceedings of the Geologists' Association 125, 317–328.

Friedman, M., Sallan, L.C., 2012. Five hundred million years of extinction and recovery: a Phanerozoic survey of large-scale diversity patterns in fishes. Palaeontology 55, 707–742.

Ginter, M., Hampe, O., Duffin, C., 2008. Chondrichthyes (Paleozoic Elasmobranchii: teeth). In Schultze, H.-P. (ed.): Handbook of Paleoichthyology 3D, 1–128. Fischer, Stuttgart & New York.

Gründel, J., Kaim, A., Nützel, A., Little, C.T.S., 2011. Early Jurassic gastropods from England. Palaeontology 54, 481–510.

Heckert, A. B., 2004. Late Triassic microvertebrates from the lower Chinle Group (Otischalkian-Adamanian: Carnian), southwestern U.S.A. New Mexico Museum of Natural History and Science Bulletin 27, 1–170.

- Kesling, R.V., 1971. *Antiquaster magruni*, a new unusual brittle-star from the Middle Devonian Silica Formation of northwestern Ohio. Contributions from the Museum of Paleontology, University of Michigan 23, 181–191.
- Klug, S., Kriwet, J., 2008. A new basal galeomorph shark (Synechodontiformes, Neoselachii) from the Early Jurassic of Europe. Naturwissenschaften 95, 443–448.
- Korneisel, D., Gallois, R.W., Duffin, C.J., Benton, M.J., 2015. Latest Triassic marine sharks and bony fishes from a bone bed preserved in a burrow system, from Devon, UK. Proceedings of the Geologists' Association 126, 130–142.
- Lakin, R., Duffin, C.J., Hildebrandt, C., Benton, M.J., 2016. The Rhaetian vertebrates of Chipping Sodbury, South Gloucestershire, UK, a comparative study. Proceedings of the Geologists' Association 127, in press.
- Lomax, D.R., Massare, J.A., 2015. A new species of *Ichthyosaurus* from the Lower Jurassic of West Dorset, England, U.K. Journal of Vertebrate Paleontology 35, 2, e903260 (doi: 10.1080/02724634.2014.903260).
- Lombardo, C., Tintori, A., 2005. Feeding specializations in Norian fishes. Annali dell'Universita' degli Studi di Ferrara. Museologia Scientifica e Naturalistica Speciale, 1–9.
- MacQuaker, J.H.S. 1994. Palaeoenvironmental significance of 'bone-beds' in organic-rich mudstone successions: an example from the Upper Triassic of south west Britain. Zoological Journal of the Linnean Society 112, 285–308.
- Mander, L., Twitchett, R.J., Benton, M.J., 2008. Palaeoecology of the late Triassic extinction event in the SW UK. Journal of the Geological Society, London 165, 319–332.
- Maron, M., Rigo, M., Bertinelli, A., Katz, M.E., Godfrey, L., Zaffani, M., Muttoni, G., 2015. Magnetostratigraphy, biostratigraphy, and chemostratigraphy of the Pignola-Abriola

- section: New constraints for the Norian-Rhaetian boundary. *Bulletin of the Geological Society of America* 127, 962–974.
- Martill, D.M., 1999. Bone beds of the Westbury Formation. In: Swift, A., Martill, D.M. (Eds.), *Fossils of the Rhaetian Penarth Group*, vol. 9. *Palaeontological Association Field Guide to Fossils*, pp. 49–64.
- Murray, J.W., Wright, C.A., 1971. The Carboniferous Limestone of Chipping Sodbury and Wick, Gloucestershire. *Geological Journal* 7, 255–270.
- Muttoni, G., Kent, D.V., Jadoul, F., Olsen, P.E., Rigo, M., 2010. Rhaetian magneto-biostratigraphy from the Southern Alps (Italy): Constraints on Triassic chronology: *Palaeogeography, Palaeoclimatology, Palaeoecology* 285, 1–16.
- Nordén, K.K., Duffin, C.J., Benton, M.J. 2015. A marine vertebrate fauna from the Late Triassic of Somerset, and a review of British placodonts. *Proceedings of the Geologists' Association* 126, 564–581.
- Plieninger, T. 1847. *Abbildungen von Zähnen aus der oberen Grenzbrecie des Keupers bei Degerloch und Steinenbronn. Jahreshefte des Vereins für vaterländische Naturkunde in Württemberg* 3, 164-167.
- Renesto, S. 2005. A possible find of *Endennasaurus* (Reptilia, Thalattosauria) with a comparison between *Endennasaurus* and *Pachystropheus*. *Neues Jahrbuch für Geologie und Paläontologie, Monatshefte* 2, 118–128.
- Reynolds, S.H., 1938. A section of Rhaetian and associated strata at Chipping Sodbury, Glos. *Geological Magazine* 75, 97–102.
- Reynolds, S.H., Vaughan, A., 1904. The Rhaetian beds of the South-Wales Direct Line. *Quarterly Journal of the Geological Society* 60, 194–214.
- Rogers, R.R., Kidwell, S.M., 2007. A conceptual framework for the genesis and analysis of vertebrate skeletal concentrations. In: Rogers, R.R., Eberth, D.A., Fiorillo, A.R. (Eds.),

Bonebeds: Genesis, analysis, and paleobiological significance. University of Chicago Press, Chicago, pp. 1–63.

- Savage, R.J.G., Large, N.F., 1966. On *Birgeria acuminata* and the absence of labyrinthodonts from the Rhaetic. *Palaeontology* 9, 135–141.
- Schoene, B., Guex, J., Bartolini, A., Schaltegger, U., Blackburn, T., 2010. Correlating the end-Triassic mass extinction and flood basalt volcanism at the 100 ka level. *Geology* 38, 387–390.
- Stanley Jr., G.D., González-León, C., Sandy, M.R., Senowbari-Daryan, B., Doyle, P., Tamura, M., Erwin, D.H., 1994. Upper Triassic invertebrates from the Antimonio Formation, Sonora, Mexico. *J. Paleontol., Mem.* 36, 1–33 (Tulsa).
- Storrs, G., 1994. Fossil vertebrate faunas of the British Rhaetian (latest Triassic). *Zoological Journal of the Linnean Society* 112, 217–259.
- Storrs, G., 1999. Tetrapods. In: Swift, A., Martill, D.M. (Eds.), *Fossils of the Rhaetian Penarth Group*, vol. 9. *Palaeontological Association Field Guide to Fossils*, pp. 223–238.
- Storrs, G.W., Gower, D.J., 1993. The earliest possible choristodere (Diapsida) and gaps in the fossil record of semi-aquatic reptiles. *Journal of the Geological Society of London* 150, 1103–1107.
- Storrs, G.W., Gower, D.J., Large, N.F., 1996. The diapsid reptile, *Pachystropheus rhaeticus*, a probable choristodere from the Rhaetian of Europe. *Palaeontology* 39, 323–349.
- Suan, G., Föllmi, K.B., Adatte, T., Bormou, B., Spangenberg, J.E., Van De Schootbrugge, B., 2012. Major environmental change and bone bed genesis prior to the Triassic–Jurassic mass extinction. *Journal of the Geological Society, London* 169, 191–200.
- Sues, H.-D., Fraser, N.C., 2010. *Triassic Life on Land: The Great Transition*. Columbia University Press, New York, 224pp.

- Swift, A., 1999. Echinoderms. In: Swift, A., Martill, D.M. (Eds.), Fossils of the Rhaetian Penarth Group, vol. 9. Palaeontological Association Field Guide to Fossils, pp. 161–167.
- Swift, A., Duffin, C.J., 1999. Trace fossils. In: Swift, A., Martill, D.M. (Eds.). Fossils of the Rhaetian Penarth Group. Palaeontological Association Field Guide to Fossils, pp. 239–250.
- Swift, A., Martill, D.M., 1999. Fossils of the Rhaetian Penarth Group. Field Guides to Fossils 9. Palaeontological Association, London, 312 pp.
- Sykes, J.H., 1974. Teeth of *Dalatias barnstonesius* in the British Rhaetic. Mercian Geologist 5, 39–48.
- Sykes, J.H., 1977. British Rhaetian bone beds. Mercian Geologist 6, 197–239.
- Sykes, J.H. 1979. *Lepidotes* sp., Rhaetian fish teeth from Barnstone, Noottinghamshire. Mercian Geologist 7, 85–91.
- Tanner, L.G., Lucas, S.G., Chapman, M.G., 2004. Assessing the record and causes of Late Triassic extinctions. Earth-Science Reviews 65, 103–139.
- Thorne, P.M., Ruta, M., Benton, M.J., 2011. Resetting the evolution of marine reptiles at the Triassic-Jurassic boundary. Proceedings of the National Academy of Sciences of the USA 108, 8339–8344.
- Thuy, B., Klompmaker, A.A., Jagt, J.W.M., 2012. Late Triassic (Rhaetian) ophiuroids from Winterswijk, the Netherlands; with comments on the systematic position of *Aplocoma* (Echinodermata, Ophirolepididae). Zootaxa 7, 163–172.
- Tintori, A. 1983. *Hypsisomatic Semionotidae (Pisces, Actinopterygii) from the Upper Triassic of Lombardy (N. Italy). Rivista Italiana di Paleontologia e Stratigrafia* 88, 417–442.
- Trueman, C.N., Benton, M.J., 1997. A geochemical method to trace the taphonomic history of reworked bones in sedimentary settings. Geology 25, 263–266.

- 1 Van den Berg, T., Whiteside, D.I., Viegas, P., Schouten, R., Benton, M.J., 2012. The Late
2 Triassic microvertebrate fauna of Tytherington, UK. *Proceedings of the Geologists’*
3
4 Association 123, 638–648.
5
6
7 Vermeij, G. J. 1977. The Mesozoic faunal revolution: evidence from snails, predators and
8
9 grazers. *Paleobiology* 3, 245–258.
10
11
12 Whiteside, D., Marshall, J.E.A., 2008. The age, fauna and palaeoenvironment of the late
13
14 Triassic fissure deposits of Tytherington, South Gloucestershire, UK. *Geological*
15
16 Magazine 145, 105–147.
17
18
19
20
21
22
23
24
25
26
27
28
29
30
31
32
33
34
35
36
37
38
39
40
41
42
43
44
45
46
47
48
49
50
51
52
53
54
55
56
57
58
59
60
61
62
63
64
65

Fig. 1. Geological map of the quarries north of Chipping Sodbury, with Southfield Quarry to the west of the B4060 road, and Hampstead Farm Quarry to the east; the Rhaetic microvertebrate samples came mainly from the south-west corner of Hampstead Farm Quarry, marked with a yellow star. Key geological formations are indicated, separated into the Devonian and Carboniferous units (bottom of column) and the key Triassic–Jurassic units above. Note that there are many subdivisions in the Carboniferous Limestone, and part of the Cromhall Sandstone appears between the Clifton Down Mudstone and the Clifton Down Limestone. © Crown Copyright and Database Right 2015. Ordnance Survey (Digimap Licence).

Fig. 2. Sketch map showing the geographic disposition of the Chipping Sodbury quarries, all lying north of the town.

Fig. 3. Photographs of Hampstead Farm Quarry, a–c taken in 1984 by Mike Curtis. (a) The older, **Southfield** Quarry, showing Carboniferous Limestone overlain by Rhaetic (grass level). (b) Excavation at Hampstead Farm Quarry, showing the eroded top of the Carboniferous Limestone overlain by black sediments of the Westbury Formation. (c) Trenched section through the Westbury Formation, as measured by Mike Curtis in 1975. (d) View of the south-west corner of HFQ in 2014, showing the Carboniferous Limestone below a grassy slope that covers the Westbury Formation lying directly on top of the Carboniferous Limestone.

Fig. 4. Sedimentary logs of the Rhaetic at Hampstead Farm Quarry. (A) Log made in summer 2014, showing the main lithologies of 20 numbered samples, each spaced 20 cm

apart, and showing main lithologies. (B) Log made by Mike Curtis in 1995, showing his 10 numbered beds. The fossiliferous horizons are his beds 1 (basal bone bed) and 9.

Fig. 5. Chondrichthyan teeth from bed 9 at HFQ. (a–c) *Duffinselache holwellensis*. (a) BRSUG 29371-1-1719 5a, anterior tooth in labial view, (b) BRSUG 29371-1-1719 5a, anterior tooth in lingual view, (c) BRSUG 29371-1-1703 5b, posterolateral tooth in lingual view. (d–f) *Lissodus minimus*. (d) BRSUG 29371-1-285 2, isolated crown in lingual view, (e) BRSUG 29371-1-285(2), isolated crown in oblique occlusal view, (f) BRSUG 29371-1-285 (1), complete tooth in lingual view. (g–m) *Pseudocetorhinus pickfordi*. (g and h) BRSUG 29371-1-1581 2a, distal tooth in lingual (g) and occlusal (h) views, (i and j) BRSUG 29371-1-280 1c, medial tooth in lingual (i) and occlusal (j) views, (k and l) BRSUG 29371-1-302 (labelled by Curtis as ‘*Hybodus* sp. nov.’), a presumed anterior tooth in lingual (k) and occlusal (l) views, (m) BRSUG 29371-1-1906, a partial tooth in oblique lingual view. (n) BRSMG Cc6361, a complete gill raker tooth. Scale bar represents 1 mm for all images, except figs. d and m, for which it is 0.5 mm.

Fig. 6. Chondrichthyan teeth from bed 9 at HFQ. (a–h) *Synechodus rhaeticus*. (a and b) BRSUG 29371-1-1611, an anterior tooth in (a) lingual view and (b) labial view. (c and d) BRSMG Cc6336, an anterolateral tooth in (c) lingual and (d) labial views. (e and f) BRSMG Cc6337, a posterolateral tooth in (e) lingual and (f) labial views. (g and h) BRSMG Cc6329, a lateral tooth in (g) lingual and (h) labial views. (i and j) BRSMG Cf13491, isolated crown of *Polyacrodus cloacinus* in (i) lingual and (j) labial views. (k) BRSUG 29371-1-1575, virtually complete tooth of *Vallisia coppi* tooth in labial view. (l and m) BRSUG 29371-1-2000, an incomplete tooth of *Rhomphaiodon minor* in lingual (l) and labial (m) views. Scale bar represents 2 mm for figs. a–d, g, h, 1 mm for figs. e, f, k–m, and 4 mm for figs. i and j.

Fig. 7. Osteichthyan teeth from bed 9 at HFQ. (a and b) *Gyrolepis albertii* teeth in side view, (a) whole tooth (BRSUG 29371-1-179 2a) in side view, (b) split tooth (BRSUG 29371-1-155 6a) showing internal structure. (c and d) ‘*Birgeria*’ type *Severnichthys acuminatus* teeth (BRSUG 29371-1-236 3b and BRSUG 29371-1-996). (e) ‘*Saurichthys*’ type *Severnichthys acuminatus* tooth (BRSUG 29371-1-145). (f–h) *Sargodon tomicus* teeth, (f) molariform-type tooth (BRSUG 29371-1-1572), (g–h) incisiform-type tooth (BRSUG 29371-1-114 4k), in two views (g and h), and BRSUG 29371-1-114 4k (h). (i and j) *Lepidotes* sp. teeth (BRSUG 29371-1-114(4k) and 29371-1-1555). (k) Morphotype O5, durophagous fish tooth plate (BRSUG 29371-1-2001). Scale bar represents 0.5 mm for all photographs except (c) for which it represents 1 mm.

Fig. 8. Neoselachian vertebrae from bed 9 at HFQ, in anterior view and lateral views. (a and b) Morphotype V1 (BRSUG 29371-1-268a). (c and d) Morphotype V2 (BRSUG 29371-1-268b). (e and f) Morphotype V3 (BRSUG 29371-1-268c). Scale bar represents 2 mm.

Fig. 9. Chondrichthyan denticles from bed 9 at HFQ; (a–j) Chimaeriform denticles; (k) placoid denticle. (a–d) Morphotype D1, two examples, in lateral (a and c) and dorsal (b and d) views (BRSMG Csb97-1a-15A; BRSMG Csbbu.sl-18-3A). (e and f) Morphotype D2, in lateral (e) and dorsal (f) views (BRSMG Csb97-19). (g and h) Morphotype D3, in lateral (g) and dorsal (h) views (BRSMG Csbbu.sl-18-3A). (i and j) Morphotype D4 (BRSUG 29371-1-1888 6a) in side (i) and occlusal (j) views. (k) Rounded placoid denticle (BRSMG Csb97-1c-39). Scale bar represents 1 mm (figs. a–h, j, k) and 2 mm (fig. i).

Fig. 10. Osteichthyan scales from bed 9 at HFQ. (a and b) *Gyrolepis alberti* scale in external (a) and internal (b) views (BRSUG 29371-1-344). (c and d) Morphotype S2 scale in external (c) and internal (d) views (BRSUG 29371-1-348). (e and f) Morphotype S3 scale in external (e) and internal (f) views (BRSUG 29371-1-351). (g and h) Morphotype S4 scale (?*Pholidophorus*) in external (g) and internal (h) views (BRSUG 29371-1-355). (i and j) Morphotype S5 scale in external (i) and internal (j) views (BRSUG 29371-1-361). Scale bar represents 0.5 mm.

Fig. 11. Osteichthyan fin ray elements from bed 9 at HFQ. (a and b) Morphotype F1 in external (a) and internal (b) views (BRSUG 29371-1-673-1a). (c and d) Morphotype F1, elongate variant, in external (c) and internal (d) views (BRSUG 29371-1-673-1b). (e and f) Morphotype F2 in external (e) and internal (f) views (BRSUG 29371-1-677-1). (g and h) Morphotype F3 in external (g) and internal (h) views (BRSUG 29371-1-674-1). (i and j) Morphotype F4 in external (i) and internal (j) views (BRSUG 29371-1-675-1). Scale bar represents 2 mm.

Fig. 12. Ichthyosaur teeth and vertebrae from bed 9 at HFQ. (a and b) Partial tooth (BRSMG Csb87-116ii) in two views. (c–e) Anterior vertebra (BRSMG Csb86-9) in anterior (c), lateral (d), and dorsal (e) views (f–h) Dorsal centrum (BRSMG Csb85-48) in anterior (f), lateral (g), and dorsal (h) views. (i–k) Caudal vertebra (BRSMG Csb87-134) in anterior (i), lateral (j) and dorsal (k) views. Abbreviations: di, diapophysis; n.a., neural arch attachment; pa, parapophysis, r.a., rib attachment. Scale bar represents 10 mm.

Fig. 13. Ichthyosaur limb bones from bed 9 at HFQ. (a and b) Proximal portion of right scapula (BRSMGCsb89-1) in lateral/ dorsal (a) and medial/ventral (b) views. (c–f) Right

femur (BRSMG Csb85-80) in dorsal (c), ventral (d), and lateral (e) views. (f and g) Round paddle bone (BRSMG Csb89-12) in dorsal (f) and ventral (g) views. (h and i) Polygonal paddle bone (BRSMG Csb85-60) in dorsal (h) and ventral (i) views. Scale bar represents 10 mm.

Fig. 14. Plesiosaur elements from bed 9 at HFQ. (a and b) Plesiosaur tooth (BRSMG Csb89-15) in two views. (c–f) Cervical vertebra (BRSMG Csb86-277) in anterior (c), lateral (d), dorsal (e), and ventral (f) views. (g and h) Centrum (BRSMG Csb87-23) in anterior (g) and dorsal (h) views. Scale bar represents 10 mm.

Fig. 15. Tetrapod limb bones and teeth from bed 9 at HFQ. (a–d) Right femur of *Pachystropeus rhaeticus* (BRSMG Csb86-31) in dorsal (a), ventral (b), right lateral (c) and left lateral (d) views. (e and f) Indeterminate bone of an unknown tetrapod (BRSMG Csb88-14) in lateral (e) and medial (f) views. (g and h) Rib of an unknown tetrapod (BRSMG Csb89-13) in right lateral (i) and left lateral (j) views. (i and j) Morphotype TT1 tooth, possibly *Thecodontosaurus* (BRSUG 29371-1-994), in side views. Scale bar represents 10 mm (figs. a–h) and 1 mm (figs. i and j).

Fig. 16. Coprolites from the Rhaetian of HFQ. (a) Spiral coprolite showing the final whorl (BRSMG Cf15469). (b) Coprolite showing traces of passage along the gut (BRSMG Cf15471). (c) Coprolite showing osteichthyan scales standing proud of the coprolite surface (BRSMG Cf.15474). (d) Coprolite showing osteichthyan scales with a preferred orientation in the body of the coprolite (BRSMG Cf.15618). (e) Coprolite containing vertebrae of *Pachystropeus rhaeticus* (BRSMG Cf15467). Scale bar represents 5 mm (figs. a, b, e) and 2 mm (c, d).

Fig. 17. Invertebrate fossils from HFQ, including gastropods (a–g), echinoids (h–k), and ophiuroids (l–u). (a–d) *Cylindrobullina*, complete specimen (BRS Csb97-1c-2ii) in lateral (a) and apertural (b) views, and steinkern (BRSMG Csb97-1c-110) in two views (c and d). (e) *Discohelix* in ventral view (BRSMG CsbBu-s164). (f) *Promathildia* (BRSMG Csb97-1c-2i). (g) Abraded possible *Glabrocingulum* (BRSMG Csb97-1c-110). (h) Broken echinoid spine, with base (BRSMG Csb97-1c-42). (i and j) Echinoid plate (BRSMG Csb97-1c-116) in internal (i) and external (j) views. (k) Ophiuroid arm vertebral ossicle (BRSMG Csb97-1c-105). (l) Ophiuroid arm vertebral ossicle (BRSMG Csb97-1c-106). (m and n) Ophiuroid arm vertebral ossicle (BRSMG Csb97-1c-106) in proximal (m) and distal (n) views. (o–t) Ophiuroid ambulacral plates (BRSMG Csb97-1c-107). Scale bar represents 1 mm (figs. a–g) and 2 mm (figs. h–t).

Fig. 18. Comparison of relative proportions of the main faunal elements from Hampstead Farm Quarry: pie charts of (a) the entire Curtis collection (n = 26237); and (b) specimens from Bed 9 (n = 2862).

Fig. 19. Fossil counts (total numbers) from the major bone-bearing horizons through the section excavated in 2014 and 2015. Bed numbers match those from Figures 4a and 20.

Fig. 20. Changing proportions of key taxa through nine bone beds and bone-bearing layers through the thickness of the Westbury Formation at Hampstead Farm Quarry; these bone-bearing horizons are numbered according to the scheme in Figs. 4 and 19. Abbreviations: *Duff.* = *Duffinselache*; duro. = durophagous tooth plates; *Rhom.* = *Rhomphaiodon*; *Sarg.* = *Sargodon*.

Summary of counts of key taxa, and unidentifiable elements, among microvertebrates in different horizons within the Westbury Formation succession at Hampstead Farm Quarry, based on sampling in 2014–2015. Abbreviations: actinopt., actinopterygian; osteich., osteichthyan; pseudocet., pseudocetorhinid.

	HFQ- 15	HFQ- 14	HFQ- 12	HFQ- 11	HFQ -2	HFQ -1	HFQ -16	HFQ- 17	basal bone bed
Bones		1	1	1	1	1	1		7
Bone fragments	6	1	14	4	35	41			10
Actinopt. elements			2	4			1		20
Osteich. Scales	12	77	29	34	51	15	35	32	86
Durophagous fish				6					0
<i>Gyrolepis</i>	6	46	40	9	55	15	27	9	69
<i>Severnichthys</i>	5	67	72	2	112	8	15	11	222
<i>Lepidotes</i>					2				0
<i>Sargodon</i>					3				2
Denticles	18	42	84	4	22	34	8	27	52
<i>Pseudocetorhinus</i>	5	35	16		20	19	7	7	0
pseudocet. gill raker		8	160	4	2			5	0
teeth fragments									
<i>Lissodus</i>		1			3				300
<i>Rhomphaiodon</i>					3				40
<i>Duffinselache</i>						1	1		
indeterminable fish			77	2	12	38	1	25	86
teeth/fragments									
miscellaneous	113	18	273	29	70	52	91	69	122
fragments									
SUM	153	296	768	99	391	224	187	185	1016

Table 2

Summary of proportions of key taxa, and unidentifiable elements, among microvertebrates in different horizons within the Westbury Formation succession at Hampstead Farm Quarry, based on sampling in 2014–2015. In the upper table, all elements are included, and in the lower table, unidentified components are excluded, and these figures are the basis for Figure 20. Abbreviations: actinopt., actinopterygian; osteich., osteichthyan; pseudocet., pseudocetorhinid.

	HFQ-15	HFQ-14	HFQ-12	HFQ-11	HFQ-2	HFQ-1	HFQ-16	HFQ-17	basal bone bed
Bones	0.00	0.00	0.00	0.01	0.00	0.00	0.01	0.00	0.01
Bone fragments	0.04	0.00	0.02	0.04	0.09	0.18	0.00	0.00	0.01
Actinopt. Elements	0.00	0.00	0.00	0.04	0.00	0.00	0.01	0.00	0.02
Osteich. Scales	0.07	0.26	0.04	0.34	0.13	0.07	0.19	0.17	0.08
Durophagous fish	0.00	0.00	0.00	0.06	0.00	0.00	0.00	0.00	0.00
<i>Gyrolepis</i>	0.04	0.16	0.05	0.09	0.14	0.07	0.14	0.05	0.07
<i>Severnichthys</i>	0.03	0.23	0.09	0.02	0.29	0.04	0.08	0.06	0.22
<i>Lepidotes</i>	0.00	0.00	0.00	0.00	0.01	0.00	0.00	0.00	0.00
<i>Sargodon</i>	0.00	0.00	0.00	0.00	0.01	0.00	0.00	0.00	0.00
Denticles	0.11	0.14	0.11	0.04	0.06	0.15	0.04	0.15	0.05
Pseudocetorhinus	0.03	0.12	0.02	0.00	0.05	0.08	0.04	0.04	0.00
pseudocet. gill raker	0.00	0.03	0.21	0.04	0.01	0.00	0.00	0.03	0.00
teeth fragments									
<i>Lissodus</i>	0.00	0.00	0.00	0.00	0.01	0.00	0.00	0.00	0.30
<i>Rhomphaiodon</i>	0.00	0.00	0.00	0.00	0.01	0.00	0.00	0.00	0.04
<i>Duffinselache</i>	0.00	0.00	0.00	0.00	0.00	0.00	0.01	0.00	0.00
indeterminable fish	0.00	0.00	0.10	0.02	0.03	0.17	0.01	0.14	0.08
teeth/fragments									
miscellaneous	0.68	0.06	0.36	0.29	0.18	0.23	0.49	0.37	0.12
fragments									
	HFQ-15	HFQ-14	HFQ-12	HFQ-11	HFQ-2	HFQ-1	HFQ-16	HFQ-17	basal bone bed
Durophagous fish	0.00	0.00	0.00	0.29	0.00	0.00	0.00	0.00	0.00
<i>Gyrolepis</i>	0.38	0.29	0.14	0.43	0.28	0.35	0.54	0.28	0.11
<i>Severnichthys</i>	0.31	0.43	0.25	0.10	0.56	0.19	0.30	0.34	0.35
<i>Lepidotes</i>	0.00	0.00	0.00	0.00	0.01	0.00	0.00	0.00	0.00
<i>Sargodon</i>	0.00	0.00	0.00	0.00	0.02	0.00	0.10	0.00	0.00
<i>Pseudocetorhinus</i>	0.31	0.22	0.06	0.00	0.10	0.44	0.14	0.22	0.00
pseudocet. gill raker	0.00	0.05	0.56	0.19	0.01	0.00	0.00	0.16	0.00
teeth frag									
<i>Lissodus</i>	0.00	0.01	0.00	0.00	0.02	0.00	0.00	0.00	0.47
<i>Rhomphaiodon</i>	0.00	0.00	0.00	0.00	0.02	0.00	0.00	0.00	0.06
<i>Duffinselache</i>	0.00	0.00	0.00	0.00	0.00	0.02	0.02	0.00	0.00

Figure 1

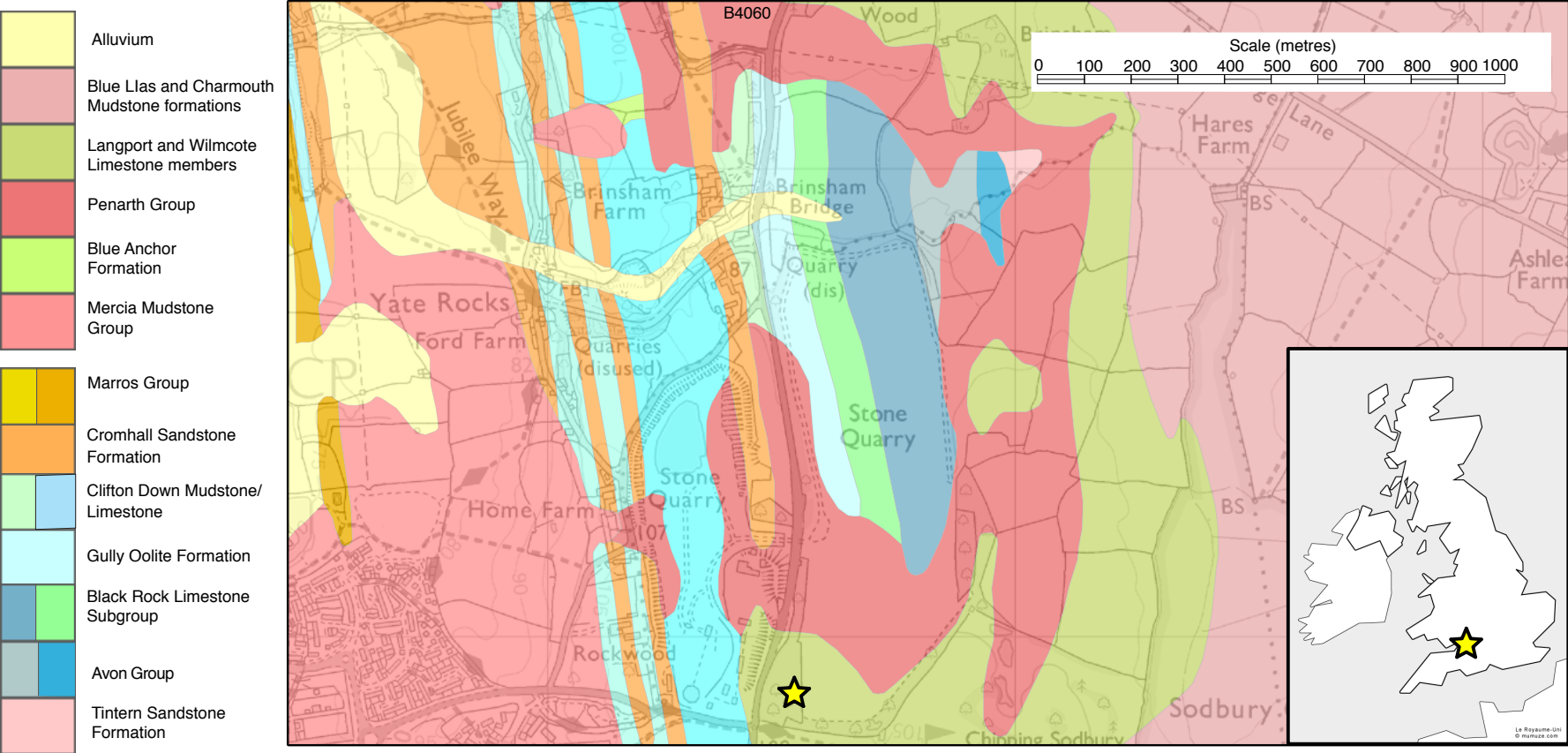


Figure 2

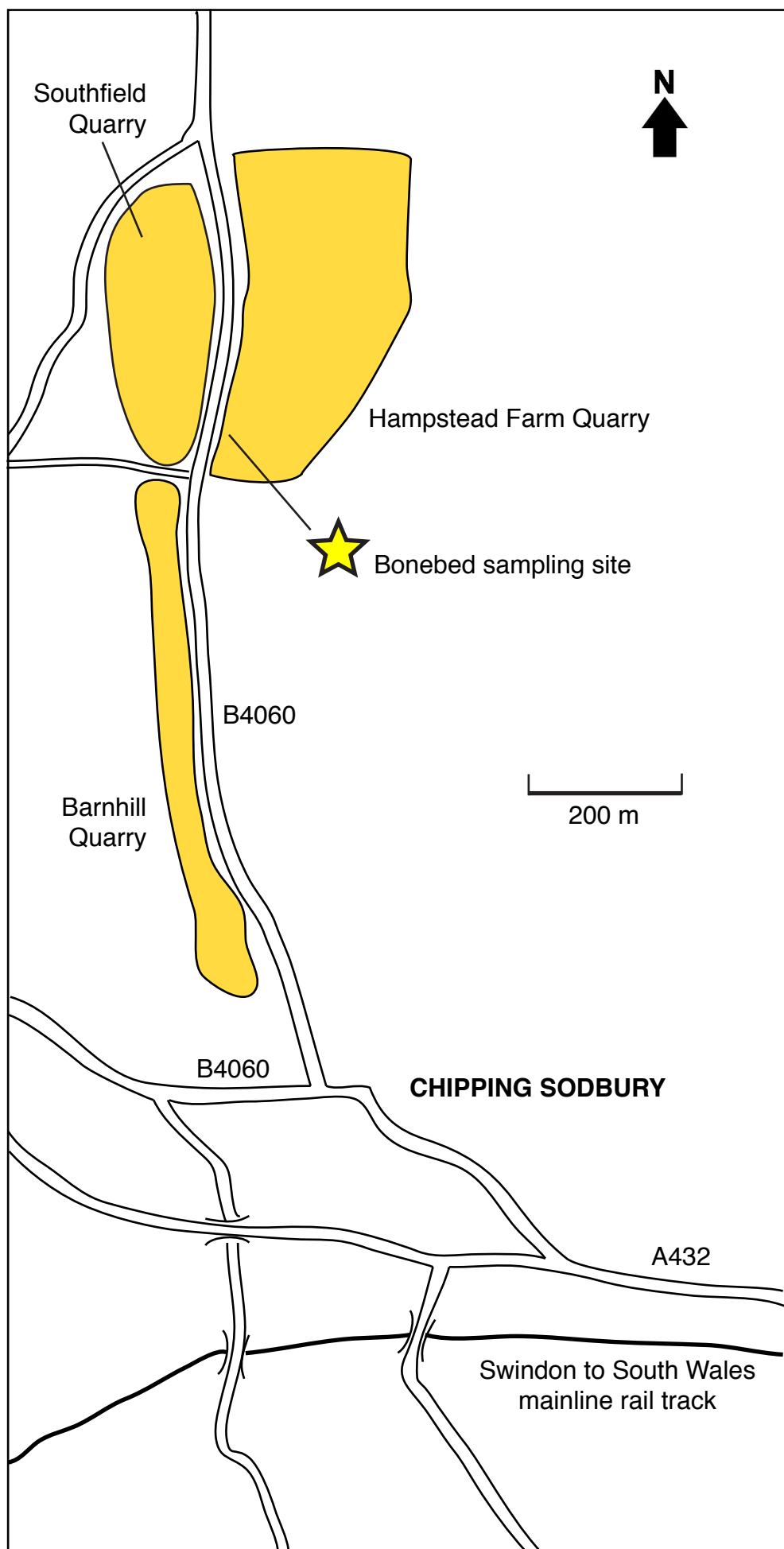


Figure 3

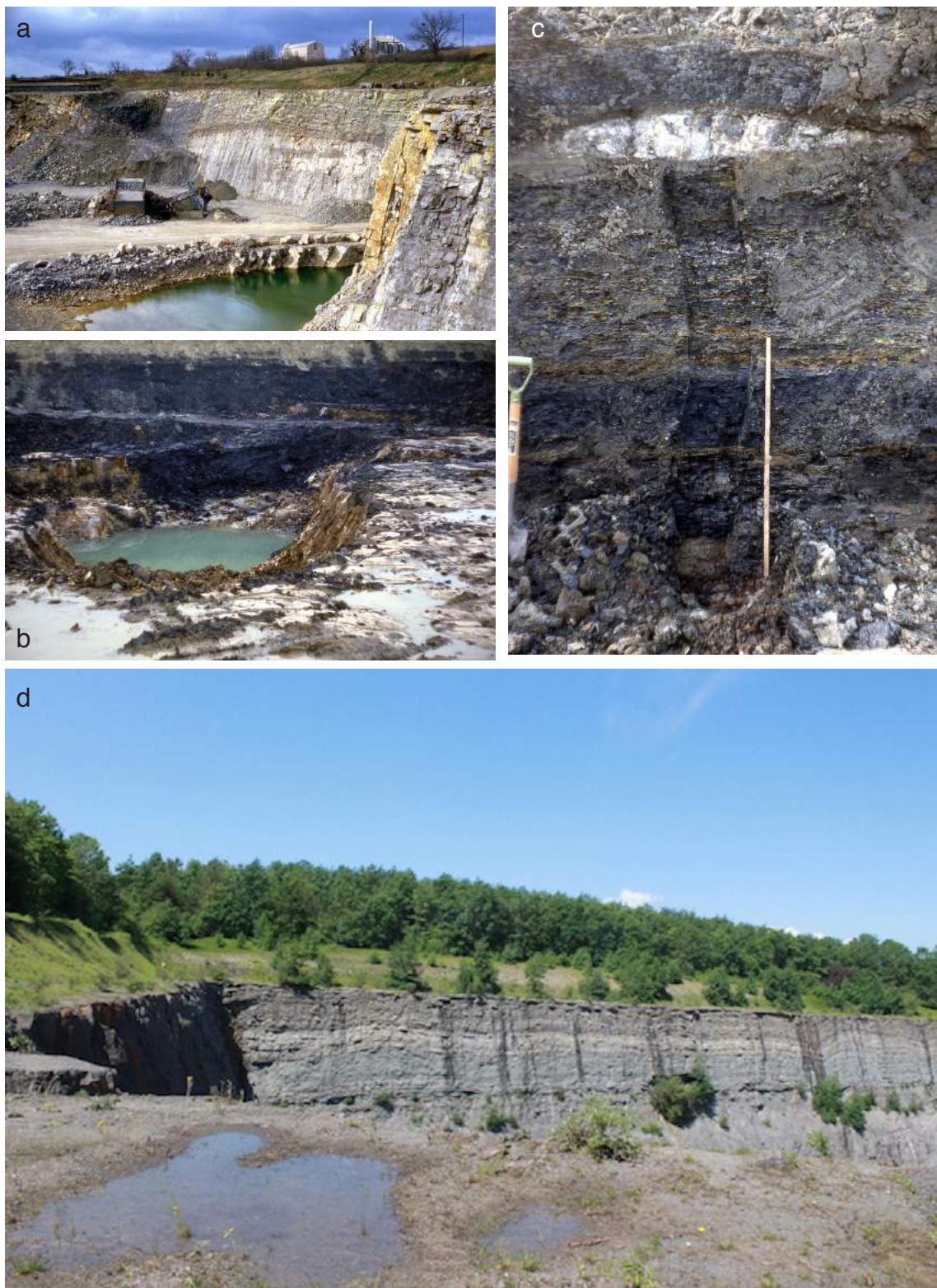


Figure 4

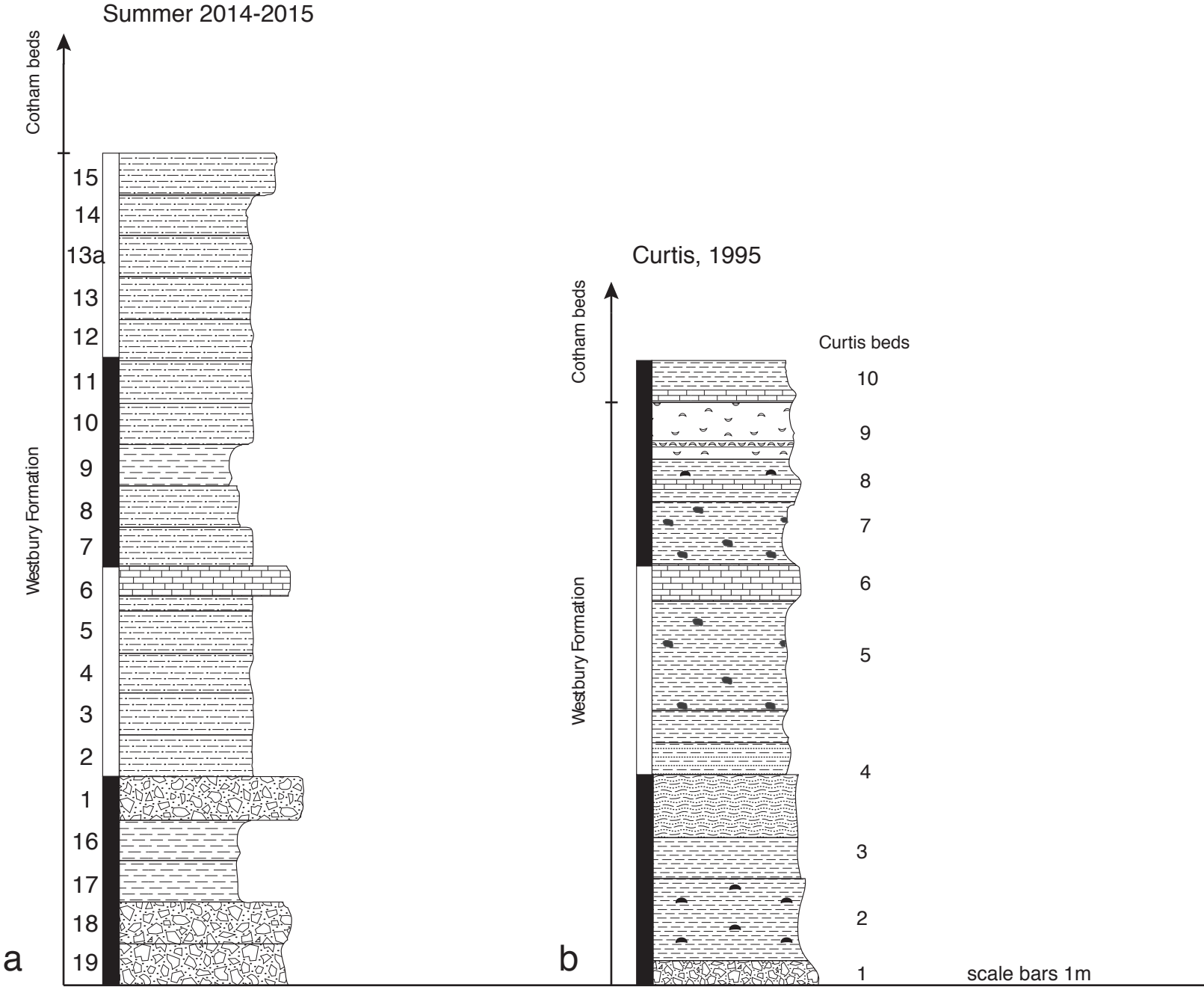


Figure 5
[Click here to download high resolution image](#)

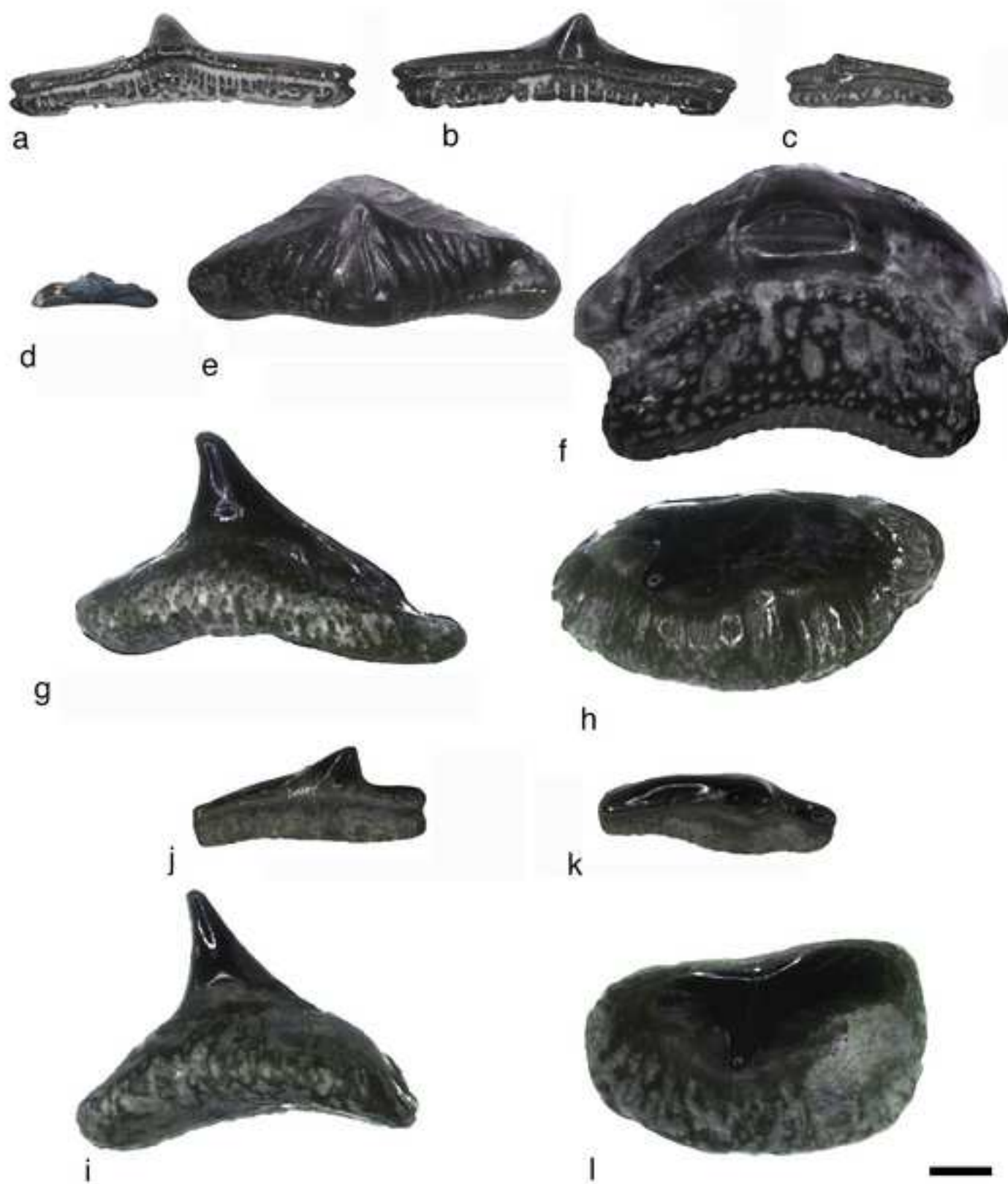


Figure 6
[Click here to download high resolution image](#)

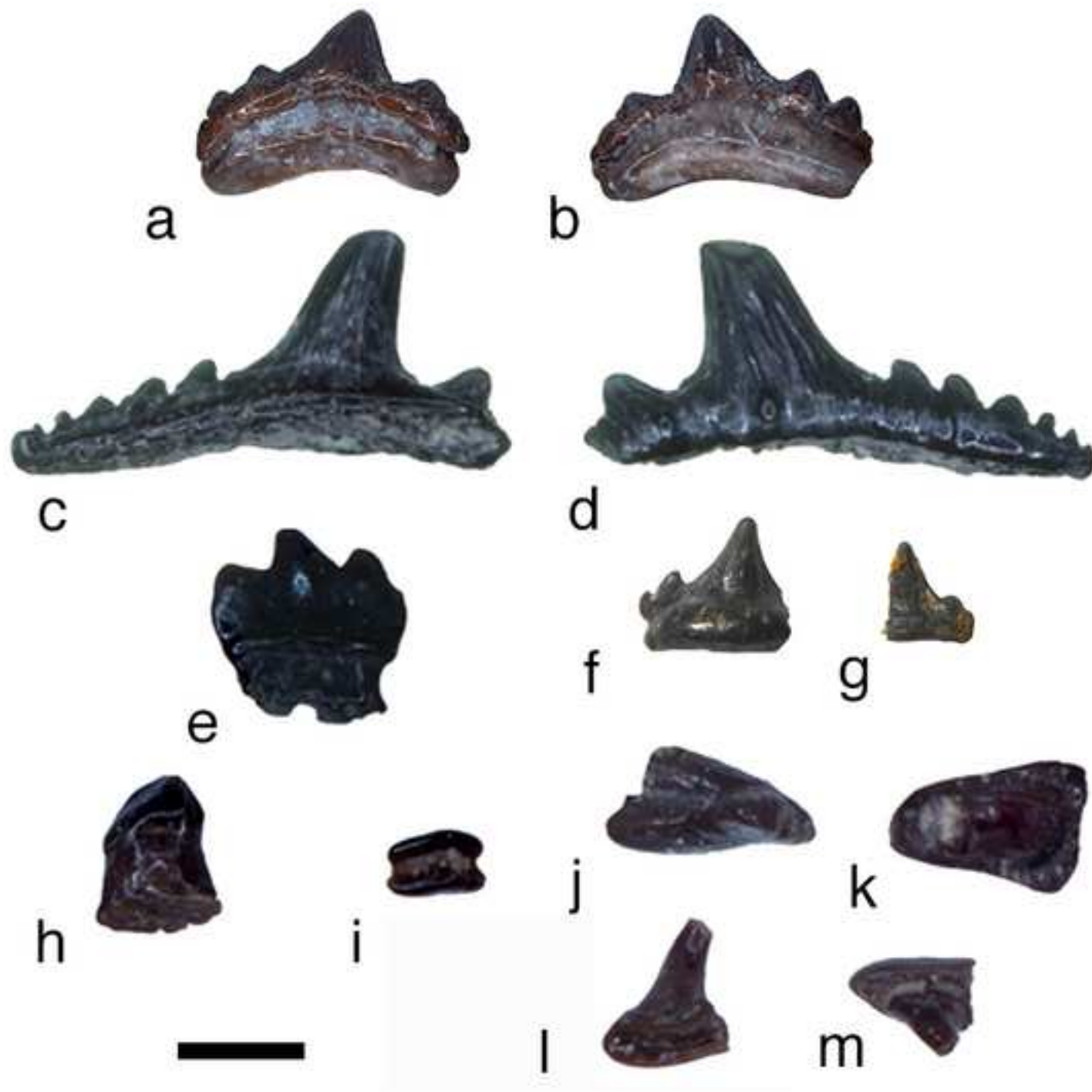


Figure 7
[Click here to download high resolution image](#)

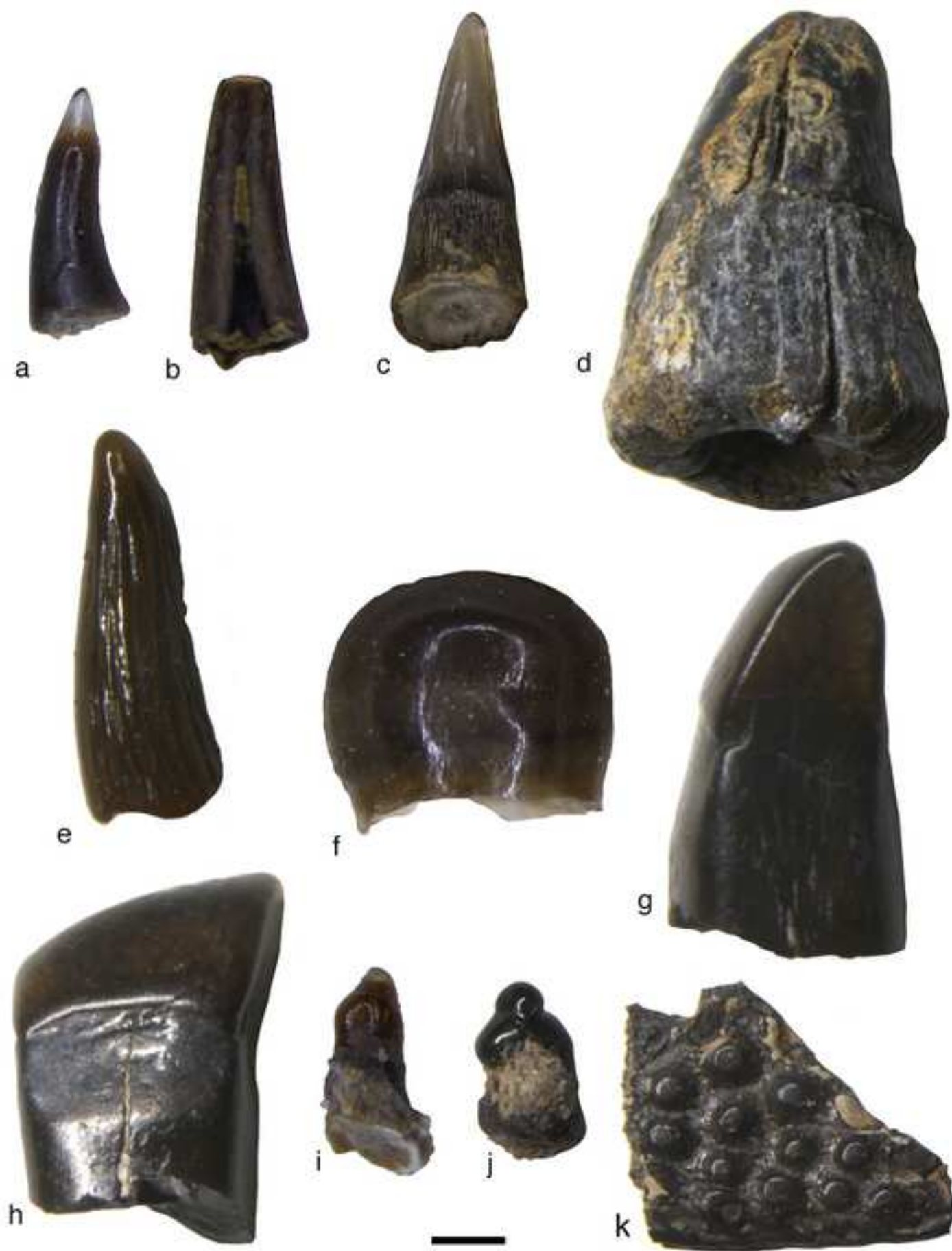


Figure 8
[Click here to download high resolution image](#)

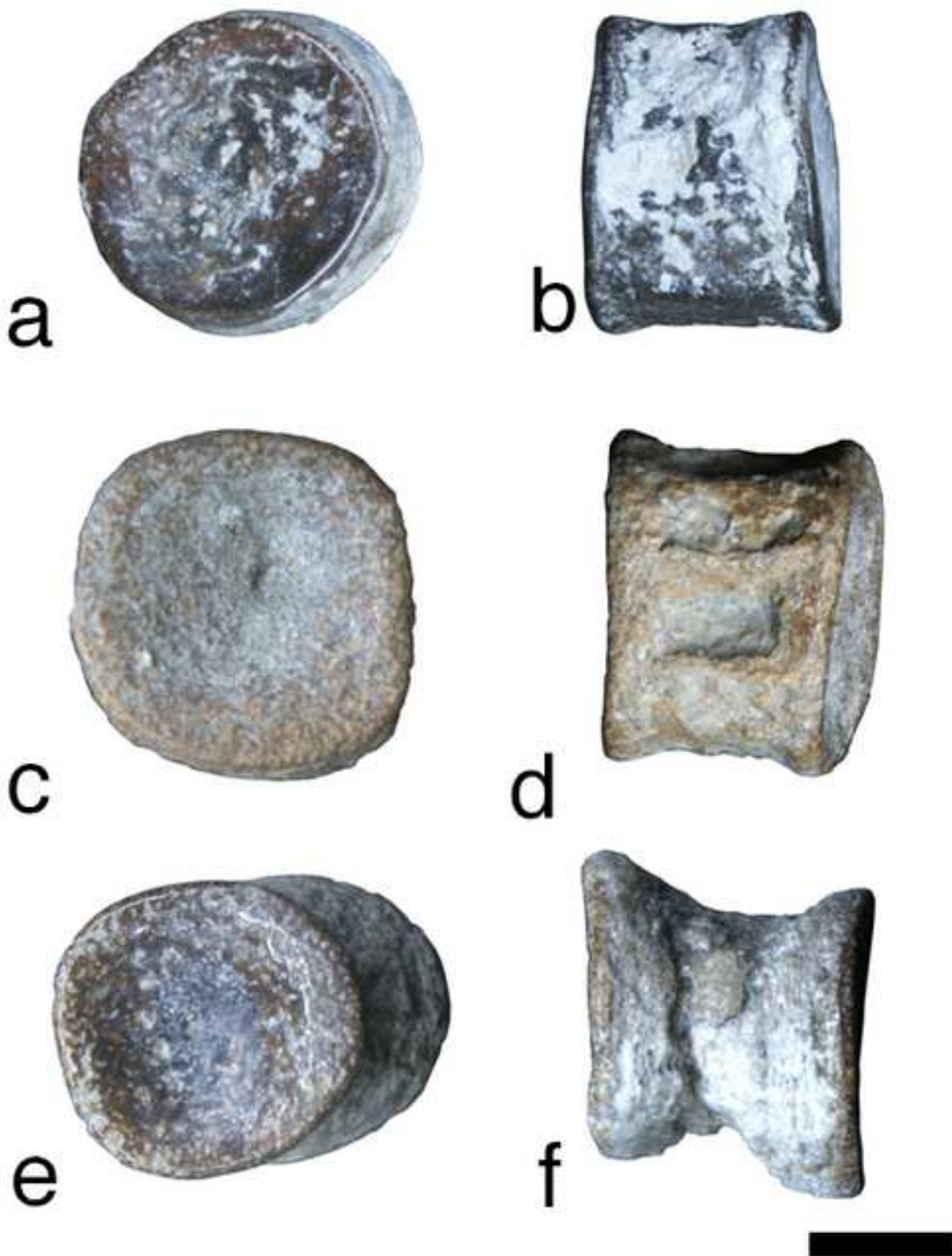
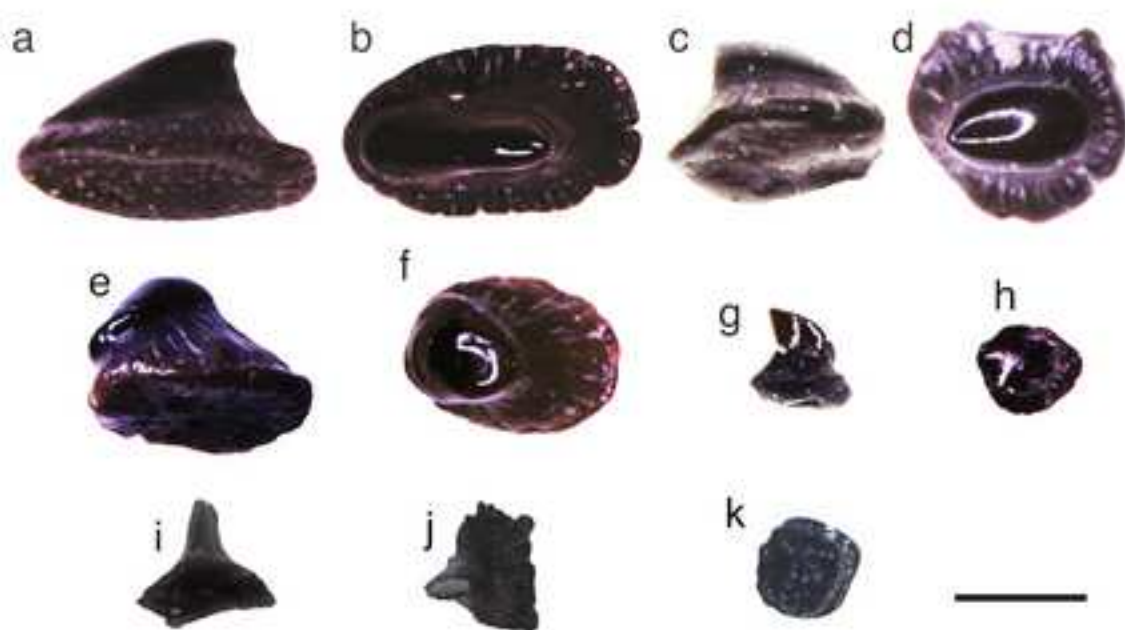


Figure 9
[Click here to download high resolution image](#)



a-h: 1 mm; i: 2 mm

Figure 10
[Click here to download high resolution image](#)

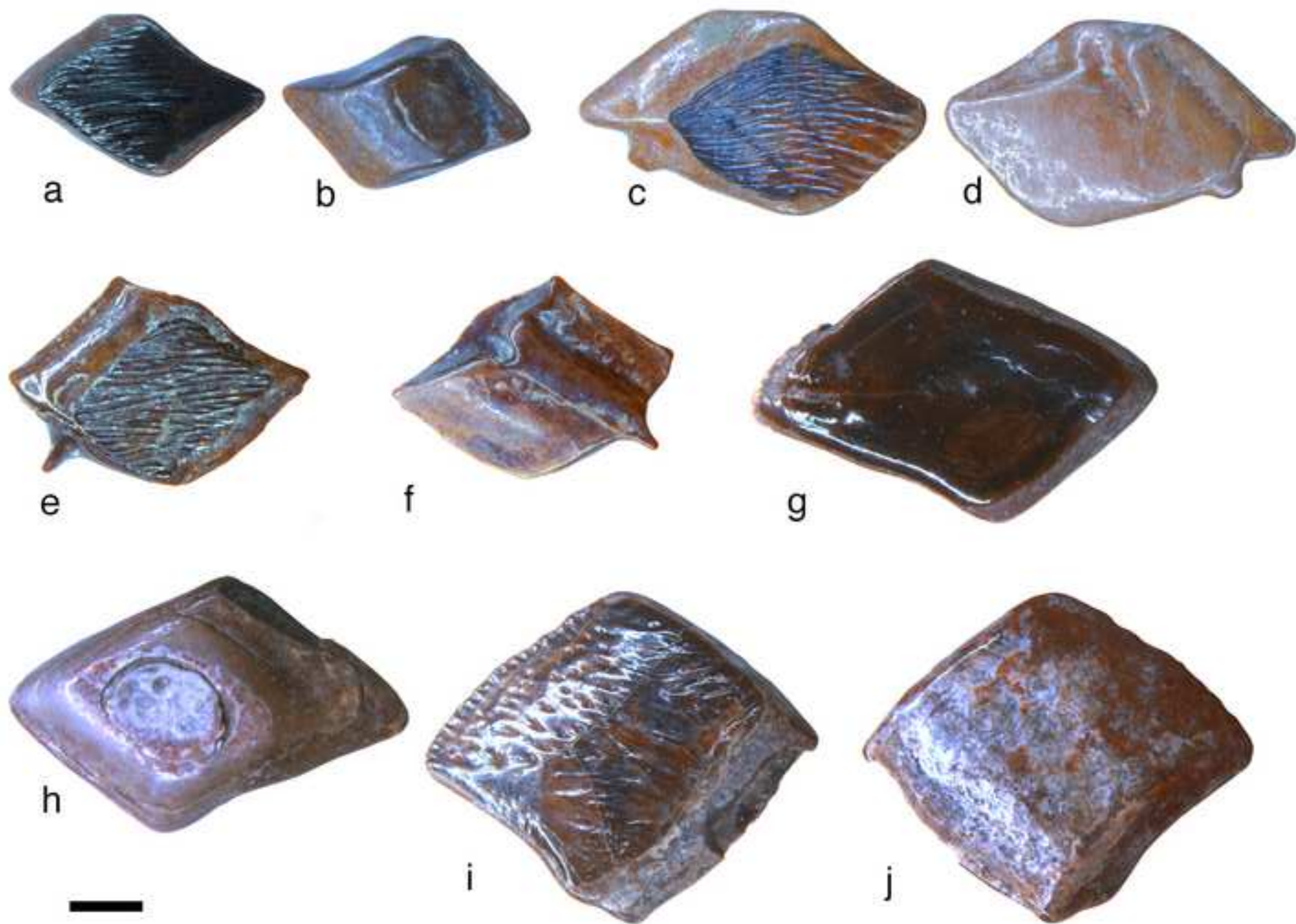


Figure 11

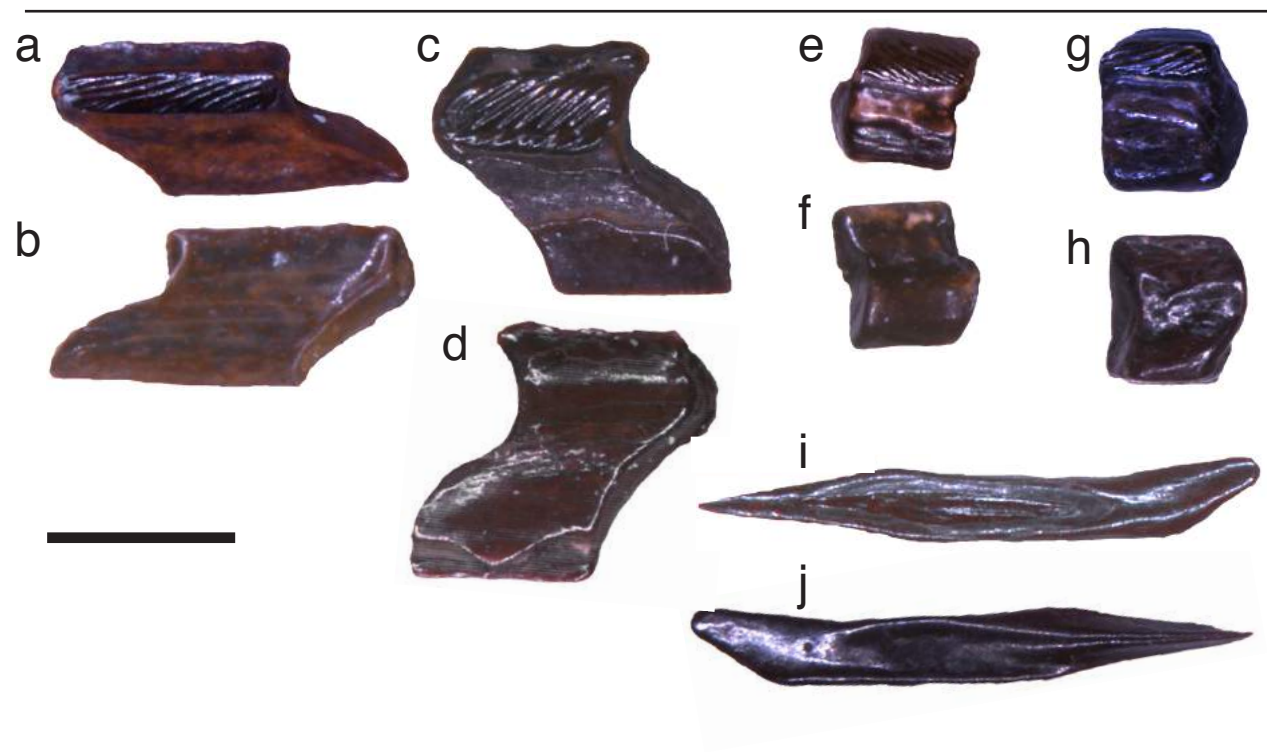


Figure 12
[Click here to download high resolution image](#)

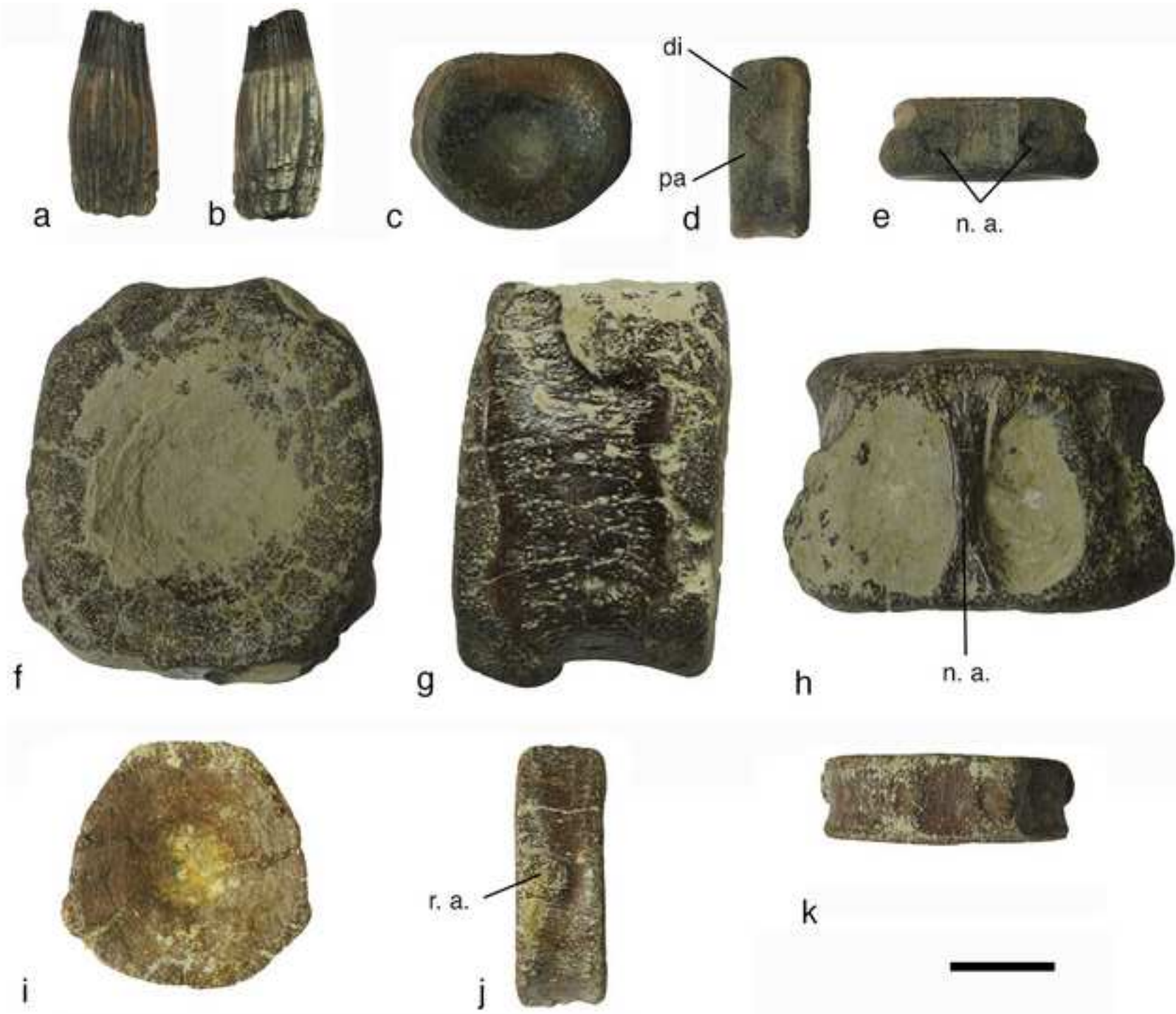


Figure 13
[Click here to download high resolution image](#)



Figure 14
[Click here to download high resolution image](#)

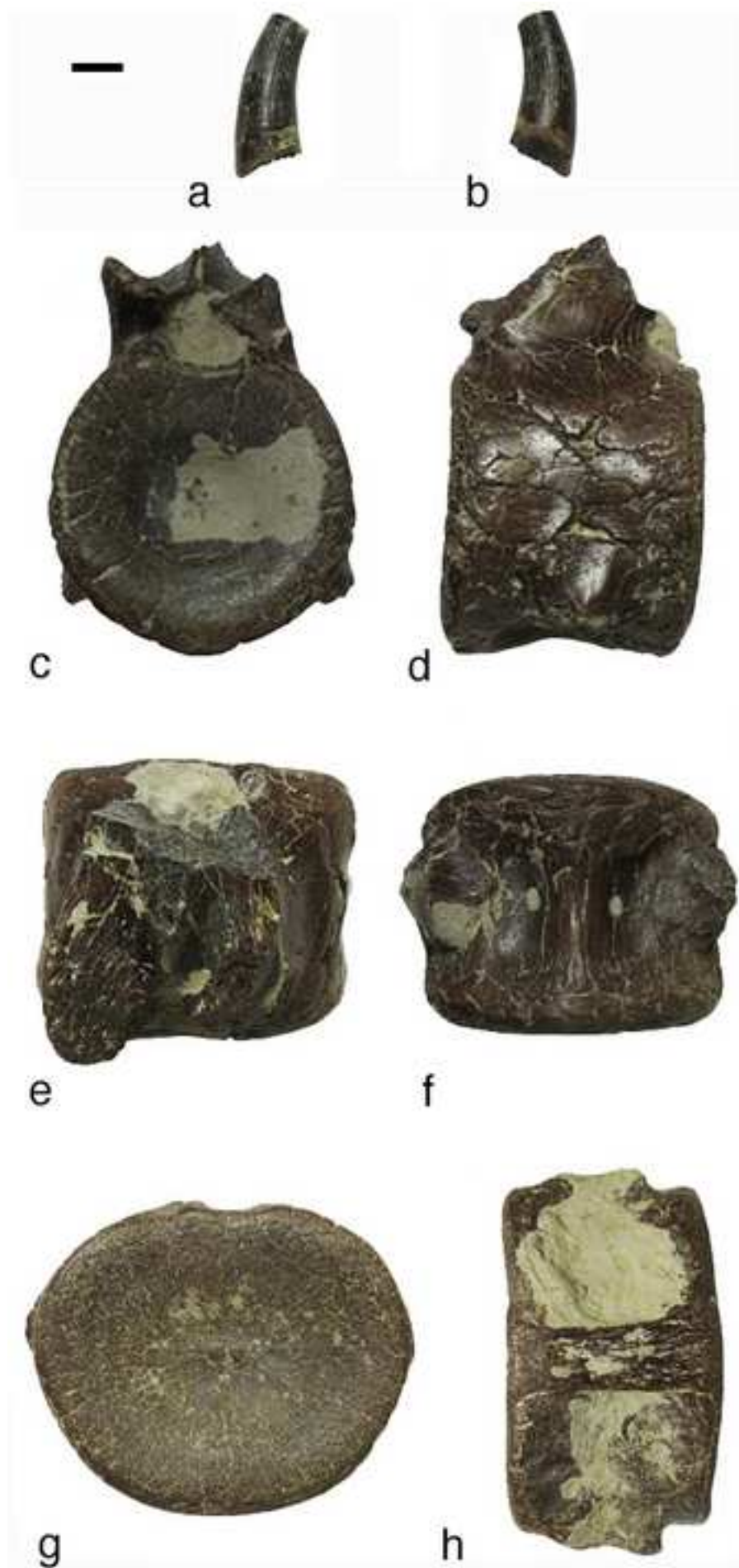


Figure 15
[Click here to download high resolution image](#)

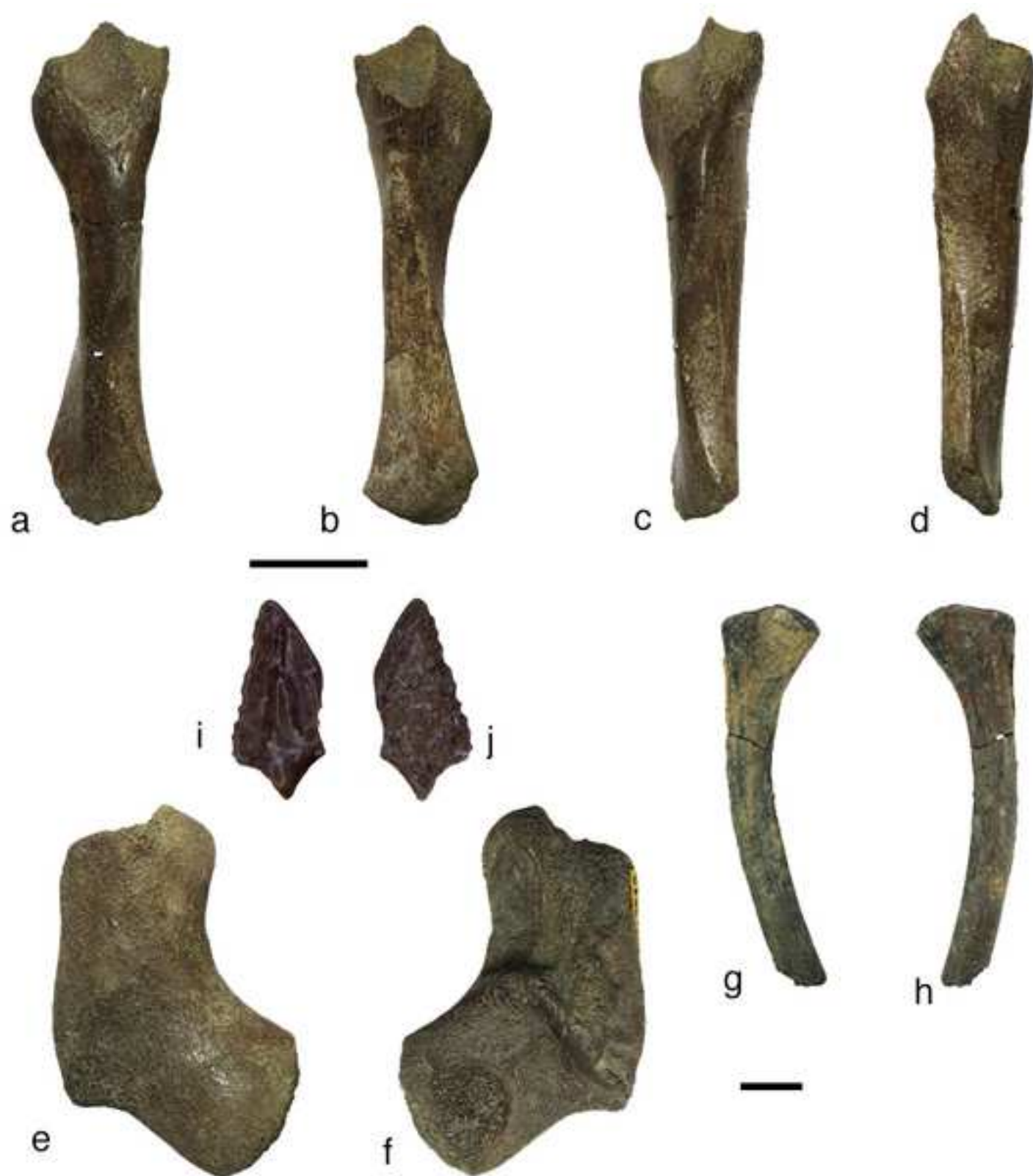
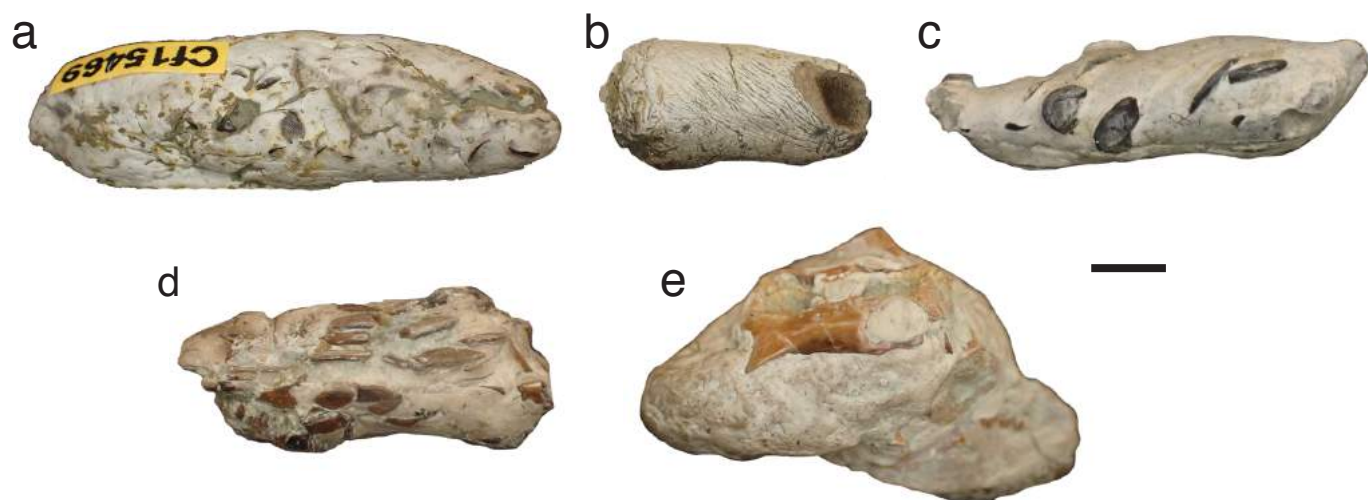


Figure 16



Scale bar is 5 mm for a, b, e; 2 mm for c, d

Figure 17

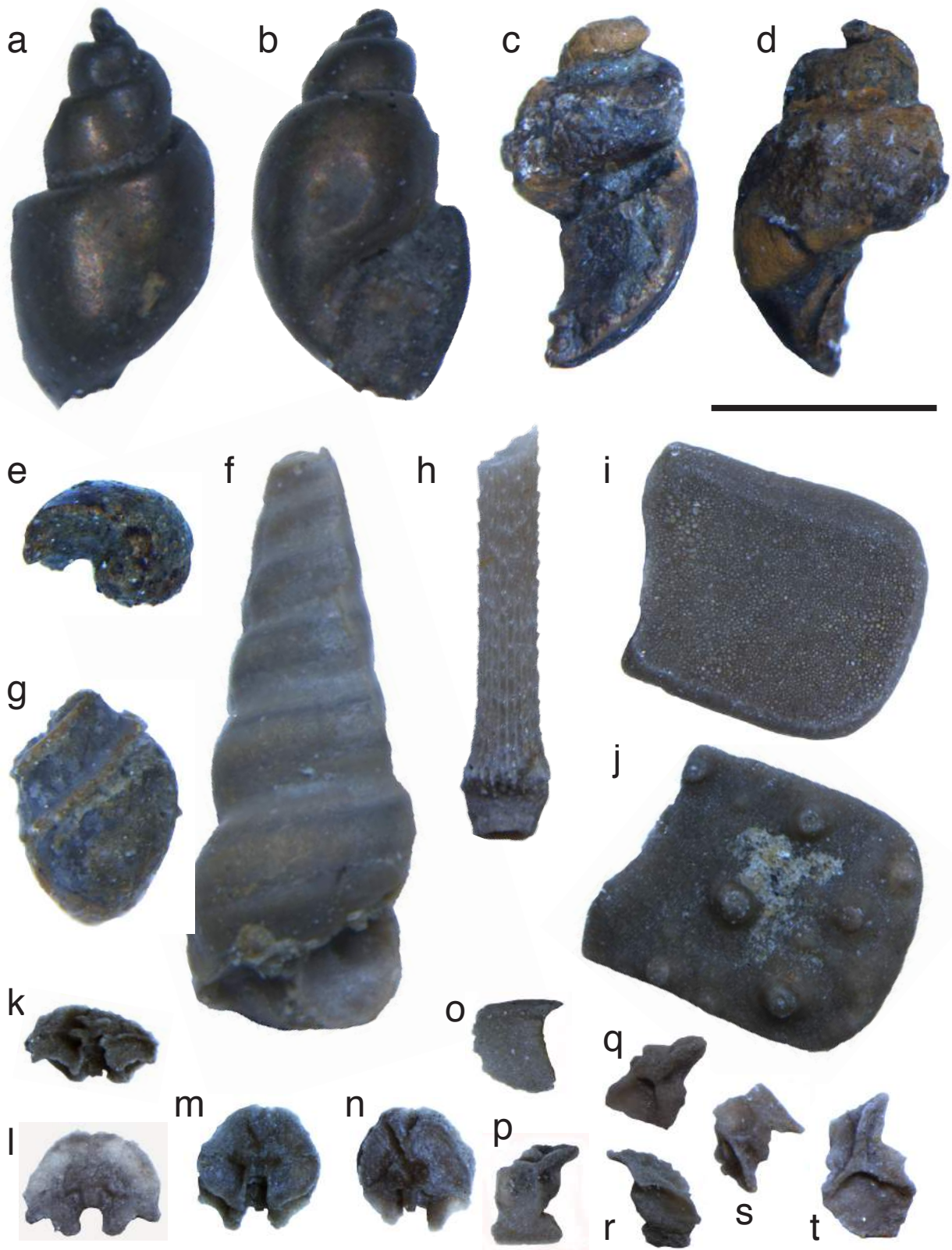


Figure 18

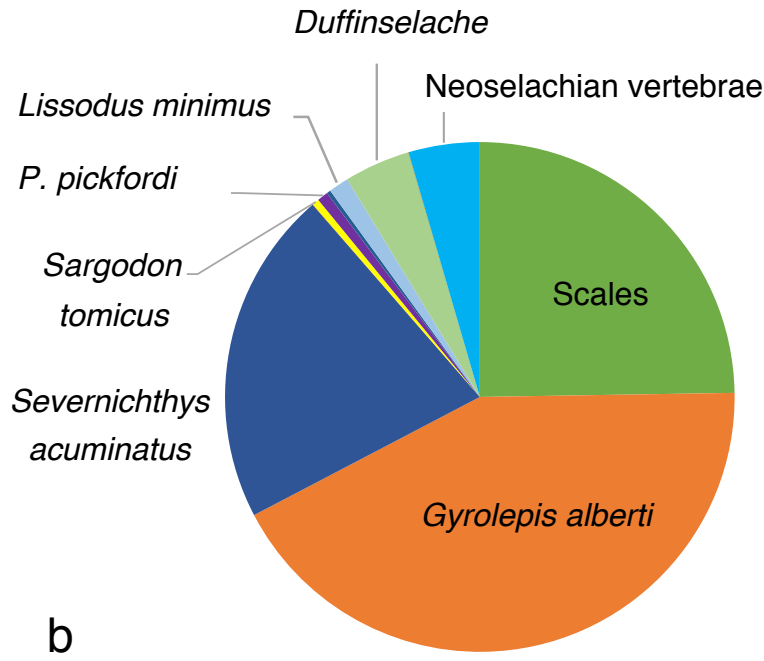
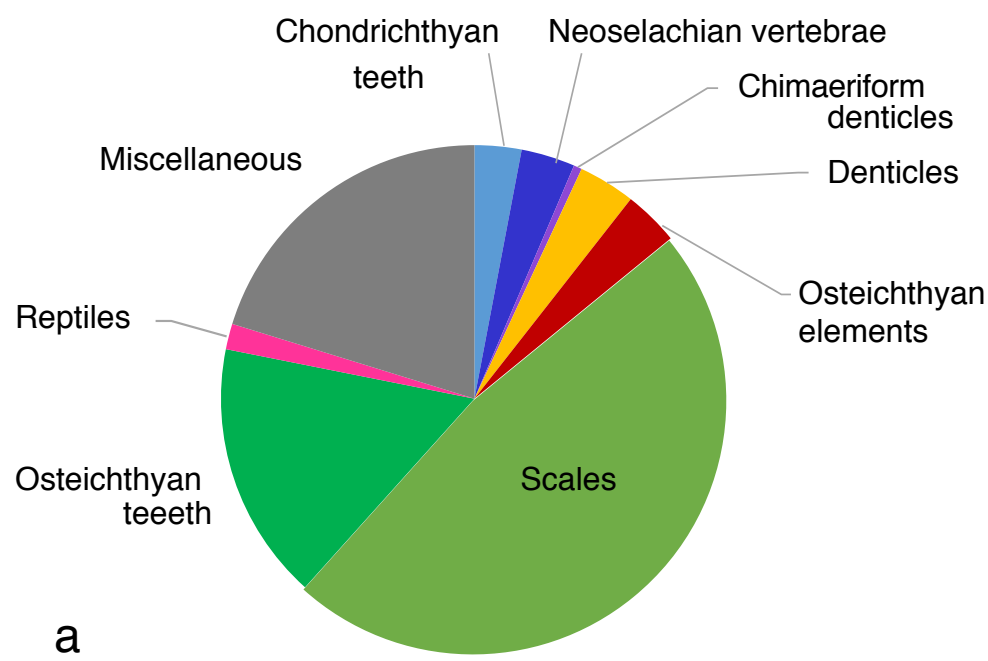


Figure 19

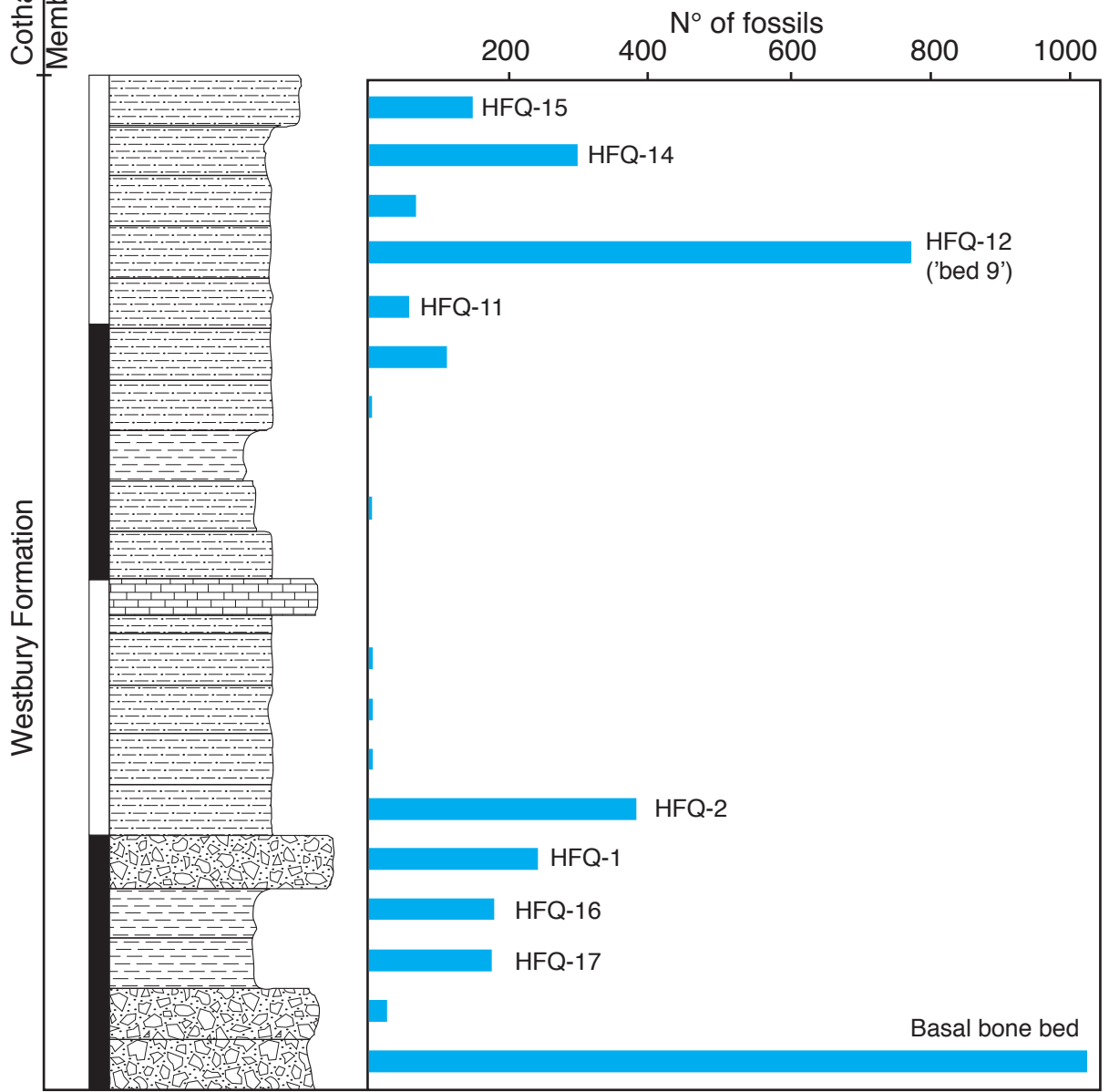
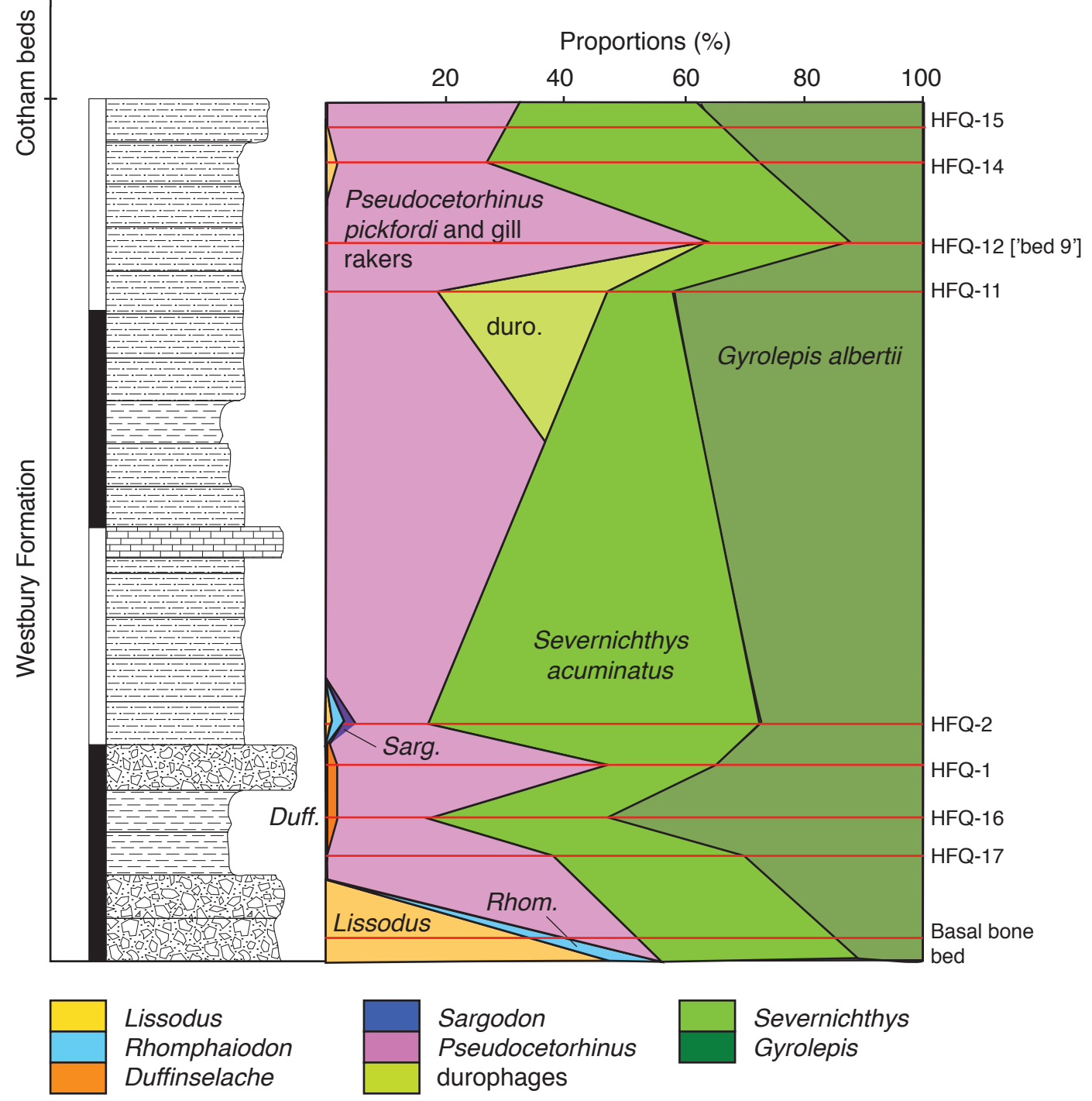


Figure 20



e-component

[Click here to download e-component: Supplement.xlsx](#)